Modelling the diffusion of pottery technologies across Afro-Eurasia: emerging insights and future research questions

Peter Jordan[1], Kevin Gibbs[2], Peter Hommel[3], Henny Piezonka[4], Fabio Silva[5] & James Steele[5,6]

[1] *Arctic Centre, University of Groningen, PO Box 716, 9700 AS Groningen, Netherlands*

[2] *Department of Anthropology, University of Nevada, Las Vegas, Box 455003, 4505 S. Maryland Parkway, Las Vegas, NV 89154, USA*

[3] *Institute of Archaeology, University of Oxford, 36 Beaumont Street, Oxford OX1 2PG, UK*

[4] *Eurasian Department, Deutsches Archäologisches Institut, Podbielskiallee 69–71, Berlin D-14195, Germany*

[5] *Institute of Archaeology, University College London, 31–34 Gordon Square, London WC1H 0PY, UK*

[6] *School of Geography, Archaeology and Environmental Sciences, University of the Witwatersrand, Jan Smuts Avenue, Braamfontein, Johannesberg 2000, South Africa*

** Corresponding author (Email: kevin.gibbs@unlv.edu)*

*Where did pottery first appear in the Old World? Statistical modelling of radiocarbon dates suggests that ceramic technology had independent origins in two different hunter-gatherer societies. Regression models were used to estimate average rates of spread and geographical dispersal of the new technology. The models confirm independent origins in East Asia (*c. *16 000 BP) and East Africa (*c. *12 000BP). The East African tradition may have later influenced the emergence of Near Eastern pottery, which then flowed west into Mediterranean Europe as part of a Western Neolithic, closely associated with the uptake of farming.*

Keywords: Neolithic transition, hunter-gatherer, agriculture, pottery, statistical model, radiocarbon dating, diffusion

1. Materials

To define land/sea boundaries we used a present-day world coastlines map, projected using the Lambert Conformal Conic projection (centred at 42.5ºN, 62ºE and with reference parallels 30ºN and 55ºN). This is an appropriate projection for the domain of interest, which has a predominant east-west orientation. To define land/sea boundaries and impose a sea mask for the distance calculation, a present-day world coastlines map was used, but extending those coastlines to 40 km offshore using a GIS buffering algorithm, to allow for dispersal and interaction by inshore and close-offshore maritime transport. This allows contact between locations separated by up to 80 km of water, and enables diffusing traits to cross most marine channels including the English Channel, the Strait of Gibraltar, and the Strait of Hormuz. For modeling purposes, additional 'bridges' were introduced to connect Japan to mainland southeast Asia and Ireland to Britain.

2. Methodology

We have developed a methodology that operates as a three-stage process. Firstly it estimates the extent of the core diffusion zone of each centre of innovation as well as the corresponding average rates of spread. These average speeds are then used to model competing/converging diffusion waves in the same domain under the first-arrival rule, i.e. after an innovation front diffuses through a neighbourhood, that neighbourhood becomes part of the relevant diffusion zone and cannot subsequently be invaded by a later-arriving competitor. This allows one to retrieve the modelled boundaries between the different diffusion zones for a given set of modelling assumptions. Lastly a series of alternative modelling assumptions, i.e. parameter sets, are explored in search of the best-fitting solution. However, because one is here trying to fit the empirical data for more than one diffusion wave, this is not as straightforward as for the single-dispersal scenario most often applied to archaeological case studies.

a. Estimating average diffusion rates

Because we could not assign *a priori* all sites in the dataset to the diffusion zone associated with a specific centre of innovation, we systematically explored the effects of imposing different cut-off distances from each centre of innovation, beyond which we would not include sites when calculating the correlation coefficient and other regression parameters. The issue is that if one makes a scattergram of date against distance from source for one of the competing diffusive processes but including sites outside its true diffusion zone, then this will yield a lower correlation between age and distance than would be the case if only sites within the diffusion zone were included. This would happen as these data points do not derive from the same underlying trend, and therefore older sites may occur at large distances from the centre of innovation, lowering the correlation coefficient. There is, therefore, an optimal distance – which we have called a cut-off distance – at which the correlation coefficient peaks before it starts to fall-off. This defines the core zone of diffusion of the innovation from a given source and is equivalent to what Ralph and Coop (2010), who consider an analogous problem in genetics, call the 'characteristic length'.

To find this cut-off distance we first model the cumulative cost surface for each cell in our domain from each centre of pottery innovation, for a given parameter set (see below). This is done using the modified Fast Marching Method described in Silva and

Steele (2014). The cost distances to individual sites in the archaeological database are then queried from the modelled cost surface, and a series of regression analyses conducted imposing cut-off distances at 1,000 equal intervals in units of cost distance. This yields, for each centre of innovation, a series of coefficients of determination, r^2, varying with cut-off distance (figure S1). The distance at which the peak r^2 value is found gives the estimate of the radius of the diffusion zone and the regression analysis using that cut-off distance yields the average rate of spread (from the inverse of the slope) as well as the average expected archaeologically-observed origination time (from the y-intercept). These are then used in the next step of the analysis.

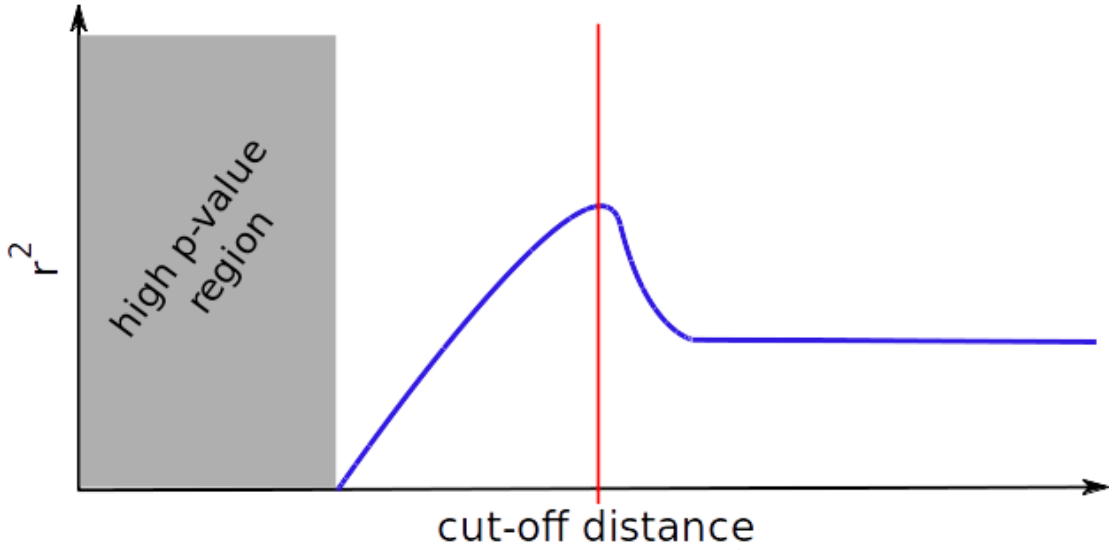

Figure S1. Plot of the coefficient of determination (r^2) against a varying cut-off distance for the regression analysis of a given diffusive process (blue line). The grey-shaded area identifies a region where a linear regression is attempted on a small number of archaeological sites, yielding untrustworthy high p-values. The red vertical line marks the cut-off distance for which r^2 peaks.

b. Modelling boundary between converging diffusion fronts

Having obtained by regression our estimates of the rate of spread as well as a y-intercept date for each of two competing/converging innovation-diffusion waves, one can then model both waves as propagating fronts subject to a 'first arrival rule'. The main restriction which the methodology imposes is that after an innovation front diffuses through a neighbourhood, that neighbourhood then becomes 'tagged' as part of the relevant diffusion zone and cannot subsequently be invaded by a later-arriving competitor. This effectively partitions the available space into the diffusion zones associated with each centre of innovation, and enables their boundaries to be defined and plotted.

The methodology employed in this study for modelling the boundary between diffusion fronts as they converge from multiple centres of innovation is a combination of two modifications of the Fast Marching Method described in Silva and Steele (2012) and Silva and Steele (2014). The former modification allows for the modelling of several competing diffusion fronts which can have different rates of spread and origination times, whereas the latter allows for heterogeneous rates of spread according to local affordances of the domain surface.

To model boosted movement of hunter-gatherer pottery from an east Asian centre of innovation through the forest-steppe region and of pottery from an African centre of innovation through the circum-Mediterranean forested biome, we have used the global present-potential biome map from Olson et al. (2001). Figure S2 highlights the biomes chosen as corridors for the two processes, namely temperate forest and temperate grassland/steppe (in green) for the east Asia-derived diffusion wave, and Mediterranean forest/woodland/scrub (in blue) for the Africa-derived diffusion wave. The Fast Marching algorithm boosts movement along these regions by multiplying the local speed by a constant factor: this is the tuneable parameter of the model. Each process has only one corridor and therefore a single tuneable parameter that determines the ratio between the speed in the corridor and elsewhere.

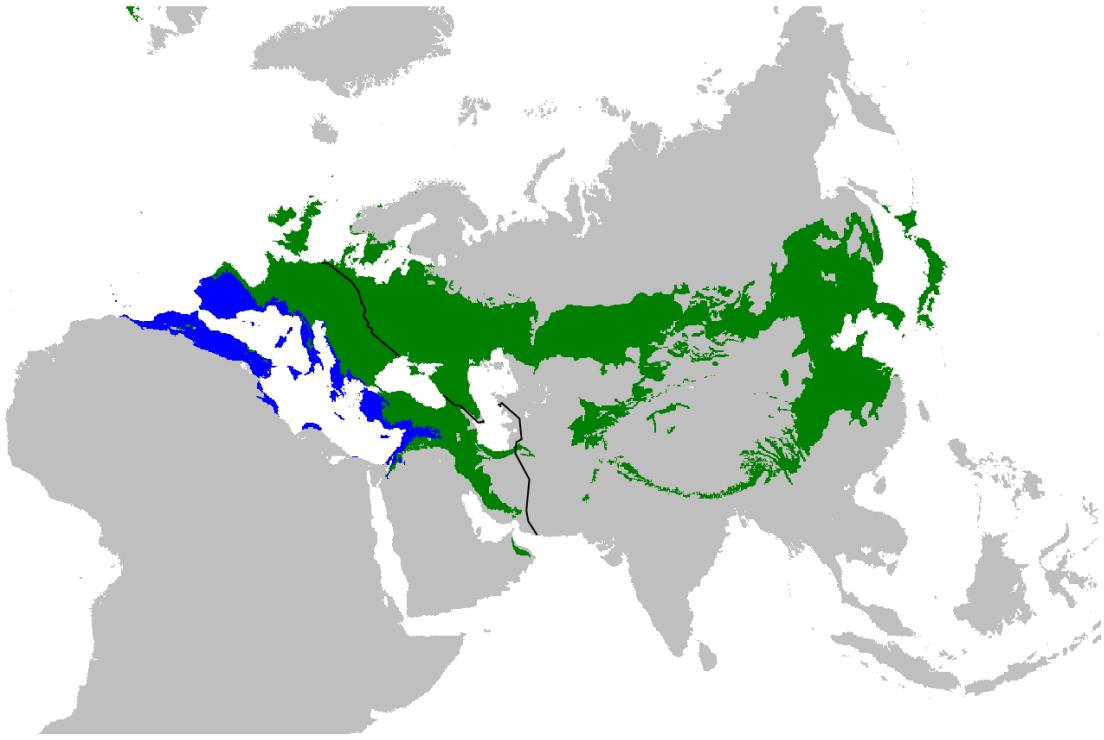

Figure S2. Map with present potential biomes, taken from Olson et al. (2001), selected as corridors for the spread of Asian pottery (temperate forests and steppe, green) and African pottery (Mediterranean forests, blue). The solid black line shows the boundary of the two diffusion waves obtained after the modelling process with boost factors of 5 for the Asia-derived wave and 7 for the Africa-derived wave (see main article), to show that it does not correspond to the boundary between the chosen biomes.

c. Optimization of the parameter set

To test our culture-ecological hypotheses about the effects of biome type on rates of diffusion of pottery technology, we assess (using the correlation coefficient) the fit of observed arrival times for pottery with distance to each site from one or other source point. Distance is a function both of the minimum Euclidean path length from point source to each site, and of the relative cost of movement across 'favourable' intervening habitat - which we quantify as an aggregated 'boost factor' (corresponding to the extent to which movement is accelerated across that part of the map). There are many possible combinations of boost factors, if we assume that

favourable habitat could have independent and varying effects on the innovation's local spatial diffusion in each of the two 'diffusion zones'. Our objective is to find the parameter set (the combination of values for each boost factor) that provides the best fit to the radiocarbon dataset, given our other modelling assumptions.

Typically an optimization algorithm, such as a Genetic Algorithm, can be used to find the parameter set that maximizes a given statistic and thus help us choose the model that has the best explanatory value. Typically, adjusted coefficients of determination, measures of residuals or information criteria have been used in archaeological applications of this (e.g. Pinhasi et al 2005; Russell, Silva and Steele 2014; Silva and Steele 2014). When dealing with more than one diffusive process one is confronted with having to maximise two such indices, irrespective of which one is chosen. In such cases, there is no single best-fitting solution but a set of them, known as a Pareto front.

A solution belongs to the Pareto front if none of the indices being optimized can be improved without degrading some of the others (figure S3). This front divides the space of possible outcomes into two regions: the feasible solutions region, containing all possible solutions, and the infeasible solutions region (which is unattainable). From a purely mathematical point of view all Pareto solutions are equally good, requiring independent discrimination to choose one solution (Branke et al 2008).

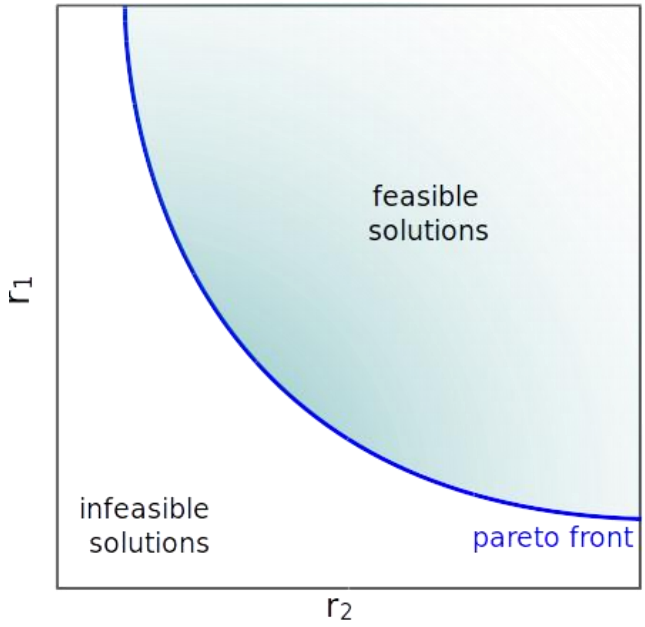

Figure S3. Outcome space plot of two independent indices, r_1 and r_2, highlighting the feasible region (green-shaded area) and the Pareto front of solutions (blue curve).

3. Results

a. Pareto front of solutions

In order to find the Pareto front for our archaeological problem we decided to make a systematic exploration of the parameter space, with the following imposition: boost factors must be integer, greater or equal than 1 and lower than 20. This limited the

number of possible combinations, and thus of computations, to 361. These were modelled and their results plotted. Figure S4 shows the obtained correlation coefficients for the two processes on the two axes; each dot corresponds to a model. The Pareto front solutions are circled with a red, blue or green circle and delimit all other solutions, which can only occupy the feasible solutions region to the right of the front.

The individual correlation coefficients of date and distance for the northern Africa-derived and east Asia-derived diffusion waves, as a function of the values assigned to the two boost factors, are shown in figure S5. The darker the shading, the greater the (negative) correlation coefficient. The Pareto solutions are identified with the colored dots. Three of these, identified in red, seem to be outliers as they appear in isolation. All other Pareto solutions occur within two clusters: one consisting of models with a boost factor of 4 or 5 for the east Asia-drived diffusion wave, the other between 9 and 11 and both with a 3 to 12 boost factor for the northern Africa-derived diffusion wave.

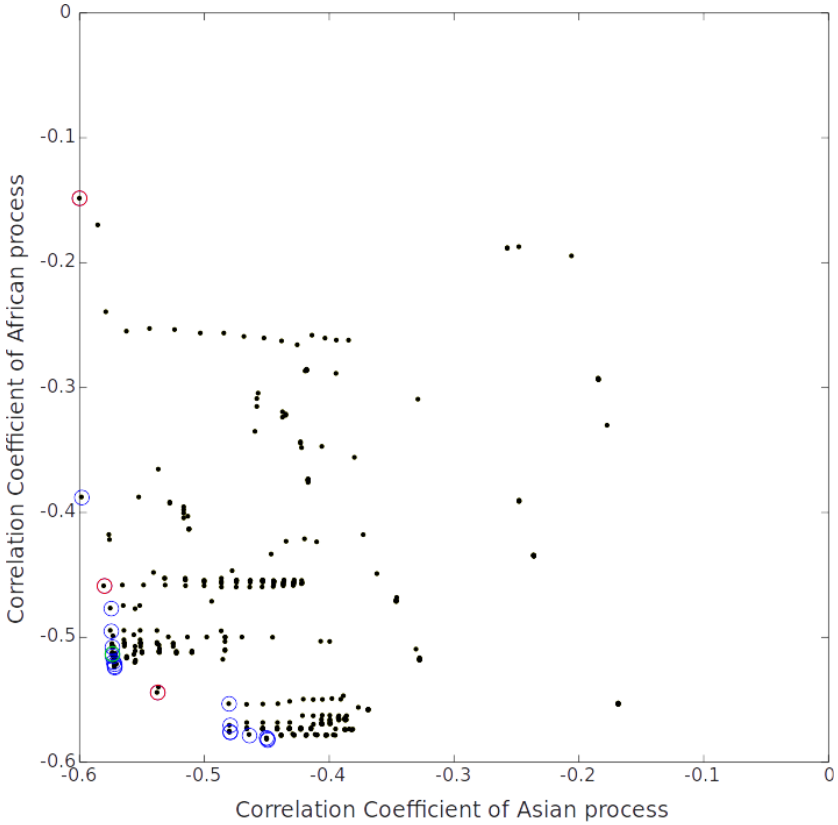

Figure S4. Outcome space plot of correlation coefficients for the African (vertical axis) and Asian (horizontal axis) processes. Each black dot represents an obtained solution, whereas those belonging to the Pareto front are marked by a coloured circle. Outliers are circled in red and the solution chosen for the figures in the main paper is marked in green, all others in blue.

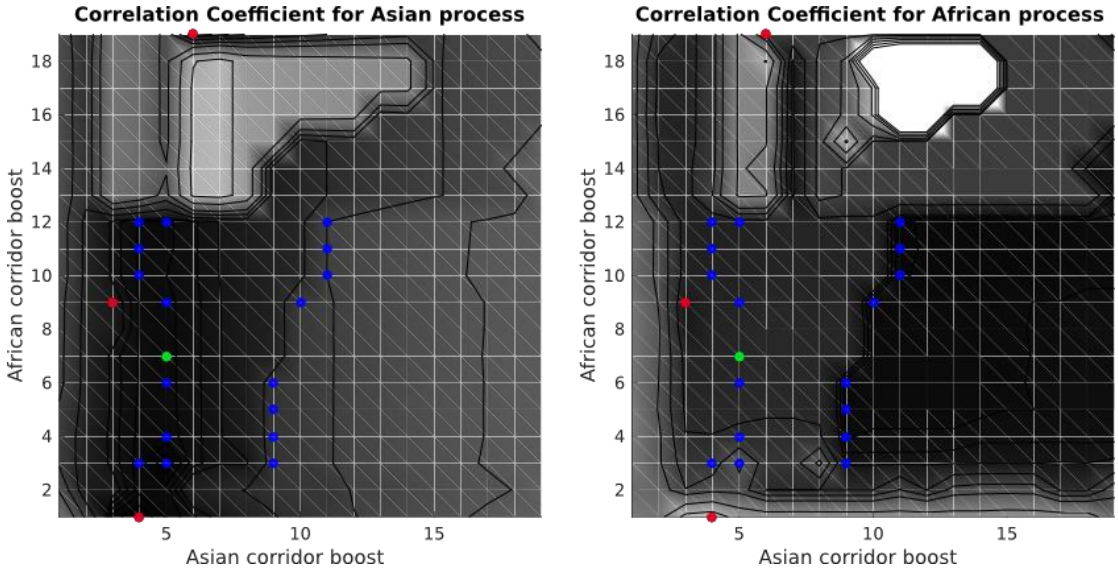

Figure S5. Parameter space contourplot of the individual correlation coefficients for the two processes with a grey colourmap (the darker the grey the lower the correlation coefficient). Pareto front solutions are indicated by a coloured dot, with the red ones indicated the outliers and the green one the one chosen for outputting figures for the main paper.

Table S1 shows the Pareto solutions with resulting correlation coefficients (Pearson and Spearman) and rates of spread in the corridor zone and elsewhere, for each diffusion wave. For comparison, the homogeneous baseline model, that is a model where there are no corridors, is also included, as well as averages and standard deviations across all Pareto-optimal solutions that indicate how well constrained these are. The Table shows that all Pareto solutions are a considerable improvement over the homogeneous model: Pearson correlation coefficients of 0.45-0.60 over 0.33 (a 36-82% improvement) and 0.39-0.58 over 0.31 (26-87% improvement) for the Asian and African diffusion zones respectively. Squaring the Pearson coefficient, to give a coefficient of determination that quantifies the covariance in the dataset, naturally increases this percentage improvement over the homogeneous baseline model. These results also show that the Spearman rank correlation coefficient, which is sensitive to non-linear correlations, is markedly greater than the Pearson coefficient for the African diffusion zone (by 22-37% in the 4x and 5x models, and 11-16% in the 9x, 10x and 11x models). This indicates a non-linear relationship between age and distance for the dispersal of pottery in the northern Africa-derived diffusion wave, which is consistent with similar findings for the spread of the Neolithic in the Mediterranean corridor (Silva and Steele 2014).

Table S1. Pareto-optimal solutions for the boost factors for the two diffusion zones, and the associated statistics for the regression slope and model goodness-of-fit. The three rows in red font correspond to the three red points on Figures S4 and S5, and represent outliers in the parameter space.

Boost factors (Asia x Africa)	Asia				Africa			
	Pearson r	Spearman rho	Speed corridor	Speed elsewhere	Pearson r	Spearman rho	Speed corridor	Speed elsewhere
1x1	-0.33	-0.37	0.31	0.31	-0.31	-0.44	0.79	0.79
4x3	-0.57	-0.58	1.18	0.29	-0.48	-0.62	1.46	0.49
4x10	-0.57	-0.57	1.18	0.29	-0.52	-0.64	3.98	0.40
4x11	-0.57	-0.57	1.18	0.29	-0.52	-0.64	4.43	0.40
4x12	-0.57	-0.57	1.18	0.29	-0.52	-0.64	4.83	0.40
5x3	-0.60	-0.62	1.25	0.25	-0.39	-0.53	1.46	0.49
5x4	-0.57	-0.59	1.25	0.25	-0.49	-0.62	1.94	0.49
5x6	-0.57	-0.58	1.25	0.25	-0.51	-0.63	2.77	0.46
5x7	-0.57	-0.58	1.25	0.25	-0.51	-0.63	3.23	0.46
5x9	-0.57	-0.58	1.47	0.29	-0.52	-0.63	3.58	0.40
5x12	-0.57	-0.58	1.25	0.25	-0.51	-0.63	5.51	0.46
9x3	-0.48	-0.55	1.15	0.13	-0.55	-0.64	1.46	0.49
9x4	-0.48	-0.54	1.15	0.13	-0.57	-0.64	1.94	0.49
9x5	-0.48	-0.54	1.15	0.13	-0.58	-0.65	2.31	0.46
9x6	-0.48	-0.54	1.15	0.13	-0.58	-0.65	2.77	0.46
10x9	-0.46	-0.55	1.15	0.12	-0.58	-0.65	4.14	0.46
11x10	-0.45	-0.54	1.15	0.10	-0.58	-0.65	3.98	0.40
11x11	-0.45	-0.55	1.15	0.10	-0.58	-0.65	4.43	0.40
11x12	-0.45	-0.55	1.15	0.10	-0.58	-0.65	4.83	0.40
3x9	-0.54	-0.53	1.15	0.38	-0.54	-0.66	4.14	0.46
4x1	-0.60	-0.63	1.18	0.29	-0.15	-0.35	0.79	0.79
6x19	-0.58	-0.59	1.17	0.19	-0.46	-0.52	5.70	0.30
Average speeds, for boost factor > 1			1.20 ±0.07	0.22 ±0.09			3.32 ±1.45	0.45 ±0.09

Looking at the speed values for the Pareto models, it is clear that, despite the different choice of parameters, these best-fitting models converged on similar solutions. The average speeds are well constrained for the east Asia-derived diffusion wave (standard deviations of 0.07-0.09 km/yr), whereas for the northern Africa-derived diffusion wave the speed along the Mediterranean corridor ranges from 1.46 to 5.51 km/yr. This range is potentially indicative of the non-linear nature of movement along this corridor, as suggested by the Spearman coefficients discussed above and elsewhere (see discussion in Silva and Steele 2014). The lowest speed outside of the corridor area, might seem low at first sight but, when considering that this speed would only kick in at northern latitudes, it is consistent with the 0.5 km/yr value proposed by Davison and collaborators in their model for the spread of the Neolithic

in Europe (Davison et al 2006, see also discussion on this model in Silva and Steele 2014).

b. "Diffusion zone" boundaries

As mentioned above in the methodology section, all of these solutions are equally good from a purely mathematical 'Pareto-optimising' point of view. Because of this, we have plotted the resulting boundaries between "diffusion zones" for all of these models (excluding the outliers) in order to observe how they cluster around a small number of variants. Figure S6 below illustrates this. For all Pareto solutions the boundaries are pretty much the same (within 300 kms of each other) for northern Europe and the Caucasus. This provides a very strong confidence in the location of the boundaries in these regions. As mentioned in the discussion in the main text, the boundaries in northern Europe are a close match to a discontinuity in subsistence strategy associated with pottery.

The boundaries for the Pareto solutions diverge only to the west and south of the Caspian Sea and towards south Asia. In this region they cluster around three distinct possibilities, the westernmost one occurring exclusively for models in the right cluster of Pareto solutions shown in figure S5. This occurs because of an increase in the correlation coefficient of the northern Africa-derived diffusion wave when the south Indian sites are included. However this seems to be due to a mathematical artefact and is unlikely to occur if more robust statistics, such as information criteria, were used instead of the correlation coefficient. Nevertheless, the pottery database for south Asia is scarce and poorly sampled and therefore it is difficult to evaluate the boundary in this region.

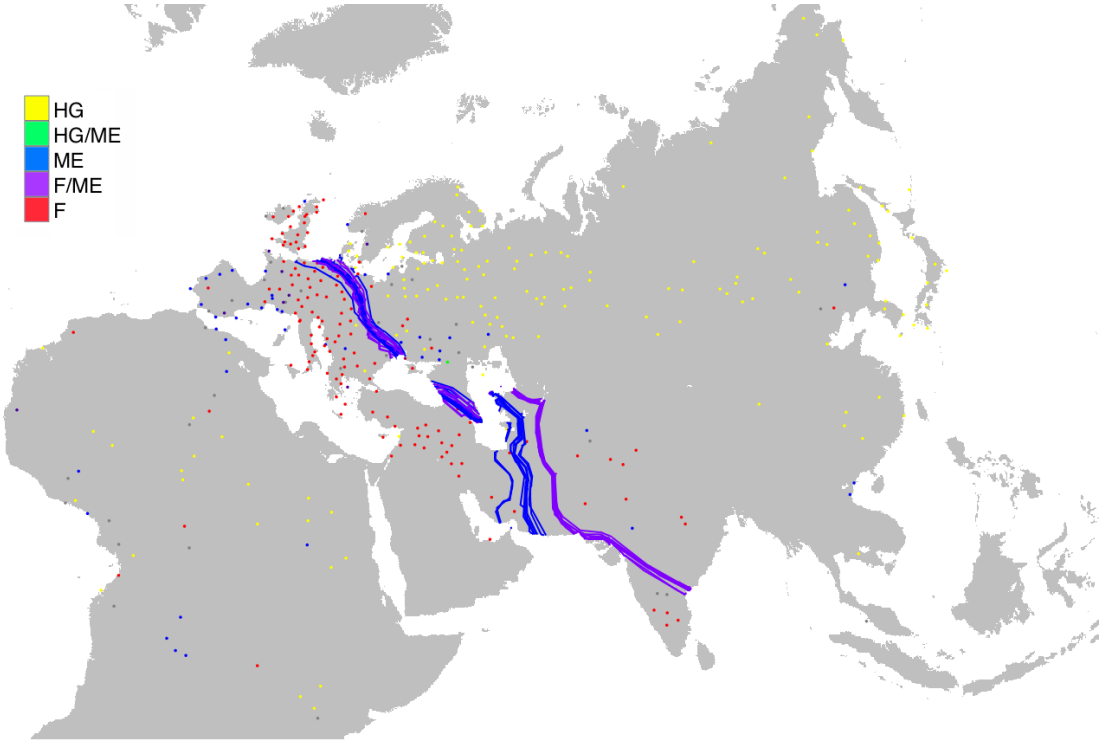

Figure S6. Map showing the boundaries for all non-outlier Pareto solutions (curved lines). The ones in blue correspond to the 4x and 5x models, whereas the purple ones correspond to the 9x, 10x and 11x models (Asian boost factors). The dots represent the sites with pottery retained for analysis, coloured in accordance to associated subsistence economy (legend: HG = hunting and gathering, ME = mixed economy, F = farming, grey = unknown or uncertain).

4. Discussion: Explanatory Power of the Model

We illustrate in Figure S7 (upper) the predicted isochrons for average age of first archaeologically-observed pottery use, for a well-fitting model with the same parameter values used to derive the boundary shown in Figure 4 (main text). This map clearly shows the accelerating effect of the boost across what we have hypothesised to have been favoured biomes. In Figure S7 (lower), we show the difference between the predicted and empirical dates for the sites in our modelled dataset (which was obtained by subtracting the values in Figure S7 [upper] from those in Figure 3a of the main text). Positive values occur where an archaeological date is older than the model predicts, while negative values occur where the archaeological dates are later than the model predicts. Comparison of this 'error map' with the distribution of modelled archaeological sites (Figure 2, bottom) reveals that some of the high values for residual error at the margins of land surfaces, where no sites exist, are likely simply due to limitations in the interpolation algorithm. In areas of the map where sites do exist and their empirical dates are 'too young', one possible explanation is simply that there has been insufficient exploration or documentation of the regional archaeological record. In both the broad regions of origination of pottery technology, however, there are sites whose dates are substantially older than the model predicts (notably, in Japan and in the Russian Far East within east Asia, and on the south western margins of the Sahara within Africa), and this most probably indicates that we have underestimated the age of origination and/or the initial local rates of diffusion of the innovation, within those broader regions. But at the larger spatial

scale, this ‘error map’ suggests that our model predicts well the arrival times of pottery technology at greater removes from those regions of innovation, particularly in the densely archaeologically-sampled record from western Eurasia.

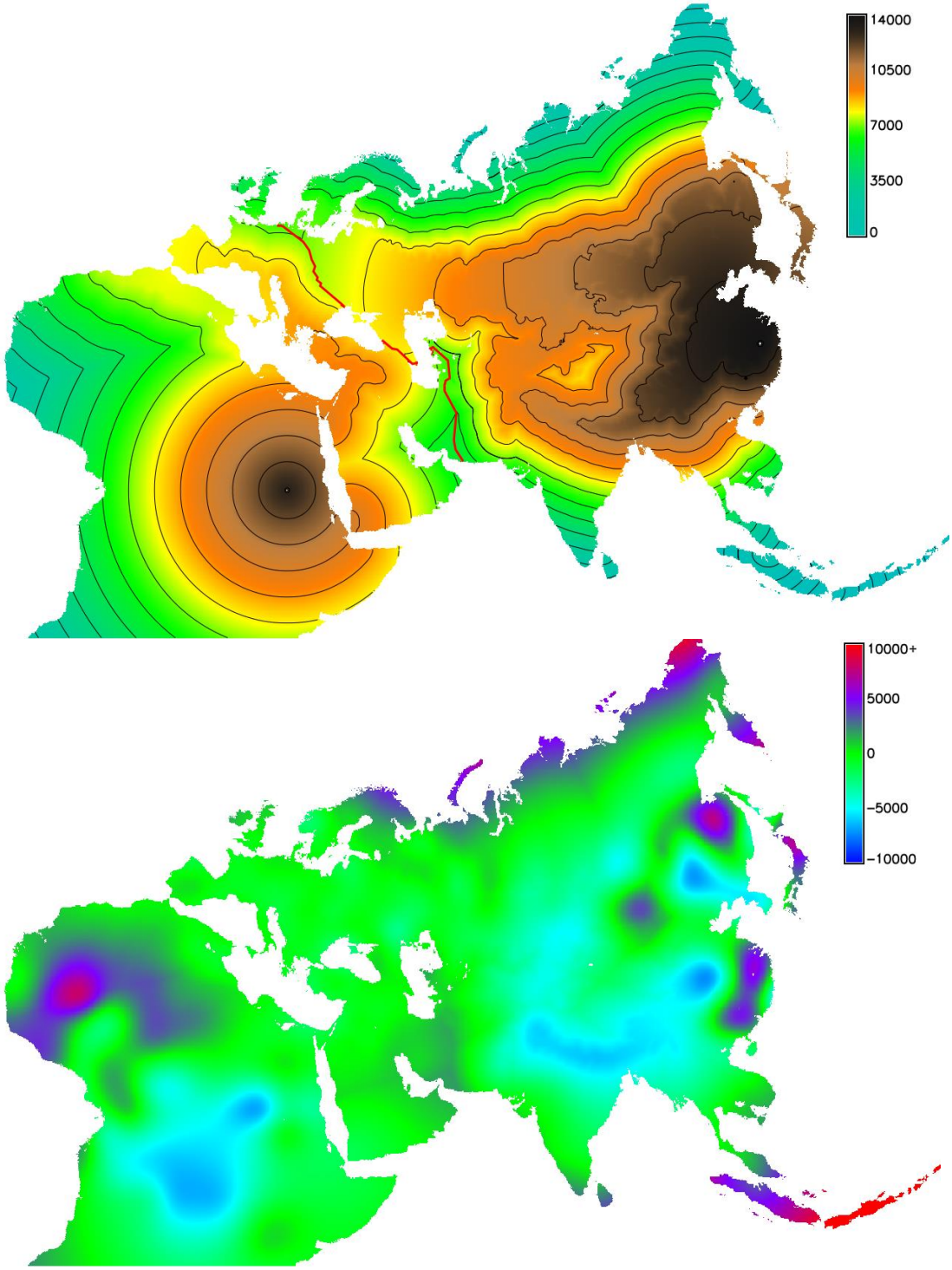

Figure S7. Modelled first arrival times for the spread of pottery from the two considered centres of innovation, with 1,000 year interval contour (top) and associated residuals, that is the difference between the empirical and the modelled arrival times (bottom), for a typical best-fitting model (the 5x7 model).

Finally, we must also recognize that while our analyses have required us to make several innovations in modeling techniques and methodology, these tools nonetheless impose further limitations. Perhaps the most obvious of these is that we have not yet implemented a dynamic representation of changing climate and global vegetation cover, even though the period under study extends from the last glacial into the early Holocene and spans a wide range of global climatic conditions. This detracts most egregiously from the value of our results for the diffusion of pottery within northern Africa. A comparison of the empirical data (Figure 3b) with the modeled arrival time surface (Figure S7) shows that the archaeological record of early pottery in Sahara and Sahel is much more widespread, and at several important sites dates to much earlier, than our model would expect. Our focus in this paper has been on accurate modeling of the diffusion of pottery-making into western Eurasia, but clearly we have also been limited by our inability to model the warm, wet Sahara and Sahel during the African Humid Period as a biome that would have acted as an additional favourable habitat for diffusion of the new technology within Africa itself (Larrasoaña *et al.* 2013). The long archaeological timespan represented by our database prevents us from using any single prehistoric land cover reconstruction map for a particular moment in time, but nevertheless it would be desirable in future work to test the sensitivity of our modeled diffusion dynamics to the placement of biome and land surface boundaries, for example by comparing results obtained on a present-potential biome map to those obtained using a late-glacial or early Holocene land cover reconstruction.

References

BRANKE J., K. DEB, K. MIETTINEN & R. SLOWINSKI (ed). 2008. *Multiobjective optimization: interactive and evolutionary approaches*. Berlin: Springer. http://dx.doi.org/10.1007/978-3-540-88908-3

DAVISON , K., P. DOLUKHANOV, G.R. SARSON & A. SHUKUROV. 2006. The role of waterways in the spread of the Neolithic. *Journal of Archaeological Science* 33: 641–52. http://dx.doi.org/10.1016/j.jas.2005.09.017

LARRASOAÑA, J.C., A.P. ROBERT & E.J. ROHLING. 2013. Dynamics of green Sahara periods and their role in hominin evolution. *PloS One* 8(10): e76514. http://dx.doi.org/10.1371/journal.pone.0076514

OLSON , D.M., E. DINERSTEIN, E.D. WIKRAMANAYAKE, N.D. BURGESS, G.V. POWELL, E.C. UNDERWOOD & K.R. KASSEM. 2001. Terrestrial ecoregions of the world: a new map of life on Earth. *BioScience* 51: 933–38. http://dx.doi.org/10.1641/0006-3568(2001)051[0933:TEOTWA]2.0.CO;2

PINHASI , R., J. FORT & A.J. AMMERMAN. 2005. Tracing the origin and spread of agriculture in Europe. *PloS Biology* 3(12): e410. http://dx.doi.org/10.1371/journal.pbio.0030410

RALPH, P. & G. COOP. 2010. Parallel adaptation: one or many waves of advance of an advantageous allele? *Genetics* 186: 647–68. http://dx.doi.org/10.1534/genetics.110.119594

RUSSELL, T., F. SILVA & J. STEELE. 2014. Modelling the spread of farming in the Bantu-speaking regions of Africa: an archaeology-based phylogeography. *PLoS ONE* 9(1): e87854. http://dx.doi.org/10.1371/journal.pone.0087854

SILVA , F. & J. STEELE. 2012. Modeling boundaries between converging fronts in prehistory. *Advances in Complex Systems* 15: 1150005. http://dx.doi.org/10.1142/S0219525911003293

– 2014. New methods for reconstructing geographical effects on dispersal rates and routes from large-scale radiocarbon databases. *Journal of Archaeological Science* 52: 609–20. http://dx.doi.org/10.1016/j.jas.2014.04.021

Site Name	Latitude	Longitude	DateBP (uncal) ± SD	Average date cal BP (INTCAL09)	Economy	Retained?
Abingdon	51.7	-1.3	5060±130	5818	F	
Abka	21.8	31.2	8260±400	9282	HG	
Abri de la Coma Francheze	42.8	2.9	5180±60	5939	F	
Abri de la Poujade	44.1	3.2	6990±120	7822	ME	TRUE
Abri de Pendimoun	44.9	5.7	6416±58	7344	ME	
Abri de Saint Mitre	44.9	5.7	6700±130	7569	un	TRUE
Abri des Usclades	44.0	3.3	5550±70	6350	HG/ME	
Abri-du-Capitaine	43.8	6.2	6050±150	6923	ME	
Abrigo de Costalena	41.2	0.3	6420±250	7268	ME	TRUE
Abrigo de Verdelpino	40.1	-2.3	7950±150	8830	un	TRUE
Abu Darbein	17.7	34.0	8640±120	9708	HG	TRUE
Abu Tabari S02/1	17.5	28.5	4855±50	5584	ME	TRUE
Abu Tabari S02/28	17.5	28.5	4110±30	4652	ME	
Abu Tabari S02/52	17.5	28.5	4760±30	5506	ME	
Åby	58.7	16.2	4665±60	5408	ME	
Acconia	38.8	16.3	6710±80	7573	F	
Achilleion	39.3	22.4	7550±60	8352	F	
Ado-Tymovo IV	51.1	142.1	7035±40	7874	HG	
Adrara Bous X	20.4	9.0	9130±65	10321	HG	TRUE
Agios Petros	39.3	24.0	6400±80	7325	F	
Aïn Naga, Algeria	34.4	3.5	7500±220	8328	HG	TRUE
Ain Rahub	32.6	35.9	7480±90	8279	F	
Ak-Tanga, Tadjikistan	39.6	68.8	5950±380	6802	ME	TRUE
Akali	58.4	27.2	6255±100	7163	HG	TRUE
Alexandria Cemetary	50.4	35.8	5470±350	6296	HG	
Ali Kosh	32.3	47.1	7820±190	8707	F	TRUE
Almazinka	46.0	135.8	7449±39	8266	HG	TRUE
Almonda Cave	39.5	-8.6	6445±32	7367	ME	
Am Hochrain, Mold	48.7	15.7	5990±160	6855	F	
Amekni, Tamanrasset	22.9	5.3	8050±80	8918	HG	
Amguyema, Madagan Oblast	67.3	178.0	6665±110	7542	HG	TRUE
Amnya 1	63.7	67.3	6900±90	7750	HG	TRUE

Site Name	Latitude	Longitude	DateBP (uncal) ± SD	Average date cal BP (INTCAL09)	Economy	Retained?
Amsa-dong	37.5	127.5	6136±76	7035	HG	TRUE
Andreevskoe Ozero	57.0	65.9	9140±60	10322	HG	TRUE
Anebis, Area 2	17.9	34.0	8230±120	9204	HG	
Anebis, Area 3	17.9	34.0	7910±140	8783	HG	
Anebis, Area 4	17.9	34.0	8090±60	9005	HG	
Ankkapurha	60.7	26.8	6060±60	6923	HG	TRUE
Anza	41.7	22.0	7206±156	8039	F	TRUE
Apa	6.4	2.8	2670±90	2777	ME	TRUE
Apatin	45.7	19.0	7062±38	7893	ME	
Araguina-Sennola	41.4	9.2	6540±99	7442	ME	
Arakhlo I	41.5	44.7	7350±70	8160	F	TRUE
Ardcrony, Co Tipperary	52.9	-8.2	4675±35	5409	F/ME	
Argissa Magoula	39.6	22.5	7500±90	8297	F	
Arma dell' Aquila, Savona	44.1	8.0	6240±90	7136	F	
Arma di Nasino	44.1	8.1	6376±47	7316	F	
Armeau	48.1	3.4	6260±65	7170	F	
Asagi Pinar	41.7	27.2	6781±39	7630	F	TRUE
Asaviec 4	54.3	27.1	5860±50	6670	HG	TRUE
Ascott-under-Wychwood	51.9	-0.4	4890±37	5626	F	
Auvernier-Port	47.0	6.9	5075±57	5812	F	
Babshin	48.5	26.6	6200±39	7092	ME	
Bagor	25.4	74.4	5620±125	6435	ME	TRUE
Baile Herculane	44.1	22.4	7320±120	8148	F	TRUE
Balbridie	57.1	-2.4	5160±70	5913	F	
Balfarg Riding School, Fife	56.2	-3.2	5170±90	5931	F	
Balise d'Amélie	45.5	-0.9	5910±150	6754	ME	
Balloy les Reaudins	44.4	3.2	6180±90	7071	F	
Banhalli	13.7	77.2	3890±70	4315	F	TRUE
Banjica	44.5	19.1	5710±90	6510	F	
Barnhouse, Orkney	59.0	-3.2	4445±20	5085	ME	
Barsova	61.3	73.3	7500±200	8312	HG	TRUE
Barsova Gora II	61.3	73.2	7450±150	8256	HG	
Basi	41.8	8.8	7700±150	8543	ME	TRUE
Battonya-Basaraga	46.9	20.8	6580±60	7484	ME	
Baume Bourbon	44.9	4.6	6050±120	6911	ME	
Baume d'Oullins	44.3	4.5	6630±110	7513	ME	

Site Name	Latitude	Longitude	DateBP (uncal) ± SD	Average date cal BP (INTCAL09)	Economy	Retained?
Baume de Montclus	44.3	4.4	6220±100	7120	ME	
Bavans	47.5	6.7	7130±70	7952	un	TRUE
Baz'kov Ostrov	48.4	29.8	7228±33	8050	ME	
Bebensee	53.9	10.3	5680±60	6473	HG	
Beeston Castle	53.1	-2.7	5140±90	5889	F	
Bel'kachi I	60.1	133.1	5970±70	6810	HG	TRUE
Beregovaya-2	58.1	58.7	7325±40	8115	HG	TRUE
Berendeevo IIa	56.6	39.0	7270±80	8087	HG	TRUE
Berezki I	52.9	59.5	7459±109	8260	HG	TRUE
Berezovaya	60.4	44.2	8700±300	9785	HG	TRUE
Berloga	53.0	106.1	6525±100	7428	HG	
Bernashëvka	48.6	27.5	6880±100	7730	ME	
Bevilacqua	38.9	16.6	6430±90	7345	F	
Bialcz Stary	52.3	16.7	5860±50	6674	F	TRUE
Biggar Common	55.6	-3.6	5216±41	5987	F	TRUE
Billerbeck, Niedersachsen	52.9	10.9	6010±100	6864	un	
Bir Kiseiba E-79-8	22.7	29.9	9820±380	11351	HG	TRUE
Bissiang	3.0	10.0	2770±70	2886	F	TRUE
Blackpatch	54.0	-9.0	5090±130	5844	F	
Boberg	53.5	10.1	5310±31	6086	HG	
Boghead, Fochabers	57.6	-3.1	4912±53	5651	F	
Boguszewo XLI	53.4	19.0	6428±77	7352	F	TRUE
Bokuma	-0.7	21.0	2260±60	2248	ME	TRUE
Border Cave	-27.1	32.0	2010±50	1968	HG	
Boso-Njafo	0.0	18.3	2270±70	2266	ME	TRUE
Bosumpra, Ghana	6.7	0.7	5219±100	6001	HG	TRUE
Bou-Sfer, Algeria	35.7	-0.8	6680±300	7572	ME	TRUE
Bouqras	35.1	40.5	7840±60	8662	F	TRUE
Breisberg	49.4	6.3	5990±200	6854	F	TRUE
Briar Hill	52.2	-0.9	5440±110	6215	F	TRUE
Bridgemere	51.2	-2.4	4630±50	5381	F	
Bringsjord	48.2	7.1	2470±80	2544	un	
Brinzeni VIII	48.1	27.3	5360±65	6132	F	
Broken Cavern, Devon	50.5	-3.7	4949±50	5689	F	
Bronneger	52.9	6.8	5777±52	6573	ME	

Site Name	Latitude	Longitude	DateBP (uncal) ± SD	Average date cal BP (INTCAL09)	Economy	Retained?
Broome Heath	52.5	1.5	5424±117	6187	F	
Brovst	57.1	9.5	5467±38	6262	HG	
Bruchenbrücken	50.3	8.8	6390±100	7304	F	TRUE
Brunn am Gebirge	48.1	16.3	6660±75	7534	F	TRUE
Brzesc Kujawski III	52.6	18.6	6178±42	7079	F	
Bukarkurari	11.7	13.5	3205±43	3428	F	
Buraco da Pala	41.5	-7.3	5860±29	6684	ME	TRUE
Burntwood Farm R6	51.1	-1.3	4750±50	5479	F	
Bury Hill	50.9	-0.6	4625±57	5350	F	
Burzahom	34.2	74.9	4205±115	4737	F	
Byblos	34.2	35.6	7360±70	8182	F	
Bylany VII	50.0	15.3	6370±40	7312	F	TRUE
Bystrinskij Kul'egan 66	61.4	72.8	6150±210	7035	HG	
Cabranosa	37.0	-9.0	6930±60	7769	ME	TRUE
Caisteal-nan-Gillean II	56.0	-6.2	5150±380	5925	F	TRUE
Caldeirão Cave	39.6	-8.5	6870±210	7733	ME	TRUE
Cannon Hill, Brey	52.9	0.7	5270±110	6058	F	
Cap Ragnon	43.4	5.3	7833±98	8680	ME	TRUE
Capel Eithin	53.2	-4.3	5454±62	6242	F	TRUE
Carn Brea	50.2	-5.3	4999±64	5746	F	TRUE
Carnanbane, Tyrone	51.7	-5.2	4978±61	5730	F	
Carrowmore	54.3	-8.5	5750±85	6553	un	TRUE
Carwood Hill, Biggar	55.6	-3.6	4990±110	5743	F	
Casabianca/ Casterragio	42.1	9.5	6670±130	7549	ME	
Casalmoro	45.3	10.4	5810±60	6610	F	
Cashelkeelty I	51.7	-9.8	5845±100	6653	un	TRUE
Cassa di Risparmio	45.7	13.8	5610±50	6385	F	
Çatalhöyük East	37.7	32.8	8091±50	9021	F	TRUE
Caucade	43.7	7.2	6660±250	7540	F	
Cavdar	42.6	24.1	7208±52	8035	F	TRUE
Cave Gua Harriman	5.2	100.1	3450±150	3743	un	TRUE
Caverna delle Arene Candide	44.5	8.5	6871±67	7716	F	TRUE
Çayönü	38.2	39.7	8053±42	8929	F	TRUE
Cendres Cave	38.7	0.5	6730±80	7589	ME	TRUE
Ceron	44.0	5.1	5990±75	6837	ME	

Site Name	Latitude	Longitude	DateBP (uncal) ± SD	Average date cal BP (INTCAL09)	Economy	Retained?
Chabarovice	50.7	14.0	6400±120	7305	F	TRUE
Chagylly-Depe	36.9	60.5	7000±100	7826	F	TRUE
Chahai	42.0	121.6	6925±95	7771	F	
Chalagantepe	40.1	47.4	6580±60	7485	F	
Chapaievka	47.3	35.5	4850±81	5579	ME	
Chapelfield, Cowie	56.1	-3.9	4823±62	5541	F	
Char-I-mar, Afganistan	36.1	66.9	7134±74	7955	F	TRUE
Chashkinskoe Ozero VIII	59.0	56.2	6310±90	7224	HG	TRUE
Chateauneuf-Les-Martigues/La Font des Pigeons (?)	43.4	5.2	6900±100	7750	ME	
Chatelliers du Viel	46.4	-0.9	5200±110	5975	un	
Chavan'ga	66.1	37.1	5560±80	6367	HG	TRUE
Chaves Cave	42.2	3.5	6770±70	7623	ME	
Chazelle	44.3	4.2	5660±110	6470	ME	
Chekalino 4	53.9	50.9	7250±60	8079	HG	TRUE
Chemin de Naviot	48.4	6.2	6279±55	7196	F	
Cherhill	51.4	-0.1	4715±90	5439	F	
Cherkaska	50.9	39.8	5710±60	6511	ME	TRUE
Chernaya Maza	56.1	45.1	4250±45	4789	HG	TRUE
Chernaya Rechka I	61.8	36.0	6200±100	7095	HG	
Chernigovka I	44.3	132.5	10770±75	12678	HG	TRUE
Chernoe 3	61.4	73.2	7090±50	7913	HG	
Chernushka I	57.7	48.8	6870±70	7717	HG	
Ches-Tuyi-Yag	64.2	60.9	6455±40	7366	HG	TRUE
Chichery	47.9	3.5	5600±120	6405	F	
Choga Mami	33.8	45.6	6846±182	7713	F	TRUE
Choinovtyi-1	64.4	50.0	5750±70	6553	HG	TRUE
Chopanimando	25.6	81.9	4540±110	5186	F	TRUE
Clarke's Shelter	-28.9	29.2	2160±50	2177	HG	
Clava	57.5	-4.1	4983±130	5740	F	
Cocorba	14.7	-0.5	3722±33	4064	HG	TRUE
Cojoux	47.8	-2.0	5577±69	6369	F	
Collingham Shelter	-29.5	29.8	1880±45	2082	HG	
Columnata	35.5	1.6	5850±100	6663	ME	TRUE
Coma Franceze	42.8	2.9	5200±70	5980	un	
Combe Grèze	44.2	3.1	6420±18	7291	F	

Site Name	Latitude	Longitude	DateBP (uncal) ± SD	Average date cal BP (INTCAL 09)	Economy	Retained?
			0			
Combe Obscure	44.5	4.1	6400±160	7284	ME	
Coneybury Henge(Stonehenge Environs)	51.2	-1.8	5050±100	5793	F	
Coppa Nevigata	41.5	15.8	7780±320	8692	F	TRUE
Corhampton	51.0	-1.2	4790±70	5505	F	
Corycian Cave	38.5	22.5	6380±90	7309	F	
Coufin II	45.1	5.4	5260±120	6034	F	
Courthezon (Le Baratin)	44.1	5.9	6600±140	7482	F	
Coygan Camp	51.8	-4.5	5000±90	5755	F	TRUE
Cueva Chicade Santiago	39.0	-6.9	7890±180	8771	F	TRUE
Cueva de El Toro	37.0	-3.6	6540±110	7437	un	
Cueva de Nerja	36.8	-3.9	7142±115	7974	un	TRUE
Cuiry-les-Chaudardes	49.4	3.8	5964±43	6800	F	
Cuka	41.3	21.5	7680±160	8522	un	TRUE
Cyclops Cave, Yura	39.4	24.2	6837±40	7666	F/ME	TRUE
Da-But	20.0	105.7	6095±60	6976	ME	TRUE
Dabki 9	54.4	16.3	6070±40	6934	ME	TRUE
Daboya	9.5	-1.4	4235±150	4792	ME	TRUE
Dachstein 74 E4 RU (Vonesch Quarry)	48.6	7.5	6280±320	7123	F	
Daktariske 5	55.8	22.9	5530±110	6318	ME	
Dalladies	57.2	-2.2	5190±190	5958	F	TRUE
Damishliyya	36.5	39.0	7920±110	8777	F	
Darion-Colia	50.7	5.2	6240±100	7131	F	
Deer's Den, Aberdeenshire	57.2	-2.4	4918±28	5640	ME	
Delebo 2, Chad	17.2	21.3	7050±212	7912	HG	TRUE
Dereivka settlement	48.9	33.7	6240±100	7140	F	
Derriere le Village	49.4	4.0	6067±95	6944	F	
Derriere les Pres	49.1	-0.1	5560±140	6350	F	TRUE
Deszk-Olajkut	46.2	20.3	6443±46	7359	F	
Diaotonghuan	28.7	117.2	14650±2	17859	HG	

Site Name	Latitude	Longitude	DateBP (uncal) ± SD	Average date cal BP (INTCAL09)	Economy	Retained?
			10			
Dibeira West (DIW-50), Sudan	21.8	31.4	5600±200	6402	HG	
Divostin	44.0	26.9	7004±37	7847	F	TRUE
Djebel Cave, Turkmenistan	39.6	54.2	6129±76	7021	HG	TRUE
Dneboh-Hrada	50.5	15.0	6300±300	7149	F	
Dobriniöye	41.8	23.6	6650±60	7526	F	
Dombé	2.9	9.9	2540±60	2600	un	
Donja Branjevina	45.5	19.1	7155±50	7981	F	
Dooey's Cairn	55.0	-6.4	5150±90	5905	F	TRUE
Dresden-Nickern	51.0	13.8	5902±58	6727	F	
Driel Shelter	-28.7	29.3	1775±40	2208	HG	TRUE
Dudestii Vechi	44.0	20.5	6861±53	7701	ME	TRUE
Dümmer	52.5	13.2	5565±85	6364	F	TRUE
Dutovo 1	63.8	56.7	6680±50	7548	HG	TRUE
Eaton Heath, Norfolk	52.6	1.3	6256±59	7165	F	TRUE
Ebbsfleet 1	51.4	0.3	4660±150	5340	F	
Egolzwil 4	47.2	8.0	5101±54	5834	F/ME	
Eilsleben	52.2	11.2	6925±60	7767	F	TRUE
Eitzum	52.2	10.8	6480±210	7350	F	
El Biod/El Bayed	28.5	6.0	7300±200	8120	un	TRUE
El Damer	17.6	34.0	8010±120	8885	HG	
El Kowm 1	35.2	38.8	7400±45	8240	F	TRUE
El Retamar	36.8	-2.3	6780±80	7636	ME	TRUE
El'gen	53.9	108.1	6790±85	7649	HG	TRUE
Elateia	38.6	22.7	7378±48	8202	F	
Eleneva Cave	56.6	92.1	7330±35	8121	HG	TRUE
Elinelund	55.6	12.9	5320±210	6093	ME	
Elshanka 11	53.9	51.1	6820±90	7679	HG	
Elsloo	51.9	5.8	6510±100	7412	F	TRUE
En’ty 1A	61.8	51.3	5625±80	6427	HG	
Endröd No. 39	46.9	20.8	6840±110	7702	ME	
Enkapune Ya Muto	-1.3	36.3	4860±70	5593	ME	
Epona II	-0.1	11.2	2850±90	2993	F	
Erbaba	37.8	31.7	7677±111	8499	F	
Erg Tichodaïne, Algeria	26.4	6.8	6870±150	7734	F	TRUE
Ertebølle	56.8	9.2	5624±45	6400	HG	TRUE

Site Name	Latitude	Longitude	DateBP (uncal) ± SD	Average date cal BP (INTCAL09)	Economy	Retained?
Etang David	47.4	4.5	5600±120	6406	F	TRUE
Eura (Kolmhaara)	61.1	22.2	5155±60	5899	HG	
Evminka-1	50.9	30.8	4864±51	5597	F	
Ezi-Ukwu Ukpa I	5.9	7.9	4885±140	5620	un	TRUE
Fadar	15.0	-0.7	3576±40	3880	F	
Fågelbacken	59.7	16.6	5070±80	5811	ME	
Fagnigola	45.9	12.7	6570±75	7478	F	TRUE
Fairyhill	55.9	13.4	5710±70	6507	un	
Falborz II	52.6	18.8	5850±170	6675	F	
Falborz IV	52.6	18.8	6050±170	6921	F	
Fendmeilen-Vordereld	47.3	8.6	5415±60	6197	F	TRUE
Fengate	52.6	-0.2	4960±64	5711	F	
Fiorano Modenese	44.5	10.8	6555±57	7464	F	
Firlus	53.3	18.6	6020±100	6875	HG	
Flynderhage	56.0	10.2	5230±100	6018	HG	
Foeni-Salas	46.5	20.9	7080±50	7903	F	
Font Juvenal	43.3	2.4	6235±85	7132	ME	
Fontbregoua	43.6	6.2	6700±100	7565	ME	TRUE
Fornace Cappuccini	44.4	12.2	6320±60	7251	F	
Fozzigiaren (Libya)	24.8	10.4	8072±100	8968	HG	
Franchthi Cave	37.4	23.1	7704±81	8496	F	TRUE
Frankenau	47.5	16.5	5660±100	6461	F	
Frare Cave	47.5	16.5	5887±120	6718	ME	
Friedberg	50.3	8.8	6120±100	7010	F	
Frigouras	44.1	6.0	5450±100	6221	F	
Frotorp	58.1	12.8	5085±75	5815	F/ME	TRUE
Fukui Cave	33.0	129.1	12499±287	14705	HG	TRUE
Fukuotun, Chinmun Island	24.7	118.5	6310±370	7170	HG	TRUE
Gabrong, Chad	21.2	17.5	8560±120	9588	HG	TRUE
Gajiganna D	12.3	13.2	3360±80	3605	F	TRUE
Gamble's Cave	-0.6	36.1	8540±180	9578	HG	TRUE
Gao Lagoon, Ghana	5.7	0.0	5219±80	6010	un	TRUE

Site Name	Latitude	Longitude	DateBP (uncal) ± SD	Average date cal BP (INTCAL09)	Economy	Retained?
Gard III	47.7	31.2	6865±50	7704	ME	
Gasya	48.8	135.6	12960±120	15643	HG	TRUE
Geleen	52.0	5.8	6370±60	7310	F	
Gerlingen	48.8	9.1	6390±160	7279	F	
Ghalogai	35.2	72.4	4218±41	4745	F	TRUE
Gird Ali Agha	36.5	43.8	6927±63	7766	F	
Gobero, Mali	17.0	9.6	8470±40	9490	HG	TRUE
Goddelau	49.8	8.5	6315±23	7233	F	
Golubjai-1	55.0	23.0	7060±270	7928	un	TRUE
Goncharka I	49.5	134.9	12500±60	14642	HG	
Gondenans-les-Monthy	47.4	6.5	5490±140	6264	F	
Gorely Les	53.6	103.2	8444±124	9418	HG	TRUE
Gornja Tuzla	44.5	18.8	6640±75	7517	F	
Gorodsk	50.4	29.2	4551±35	5195	F	TRUE
Gospodska pecina	44.0	16.4	7010±90	7833	F	TRUE
Göttingen	51.5	9.9	6530±180	7417	un	TRUE
Grande	48.9	2.3	5260±70	6054	F	
Grapčeva	43.2	16.8	7030±60	7859	ME	TRUE
Gravholmen	69.2	29.3	6092±45	6970	HG	
Grayan-et-l'Hopital (La Léde du Gurp)	45.4	-1.1	6100±65	6992	F	
Grebenyukuv yar	48.8	30.5	6116±32	7017	F	
Greifensee	47.4	8.7	5140±35	5873	F	
Grenovka	48.1	30.5	5833±33	6645	F/ME	
Gromatukha	51.8	128.8	13269±65	16208	HG	TRUE
Gropbakkeengen	70.1	28.6	4750±150	5450	HG	
Grotta Arma dello Stefanin	44.1	8.0	6610±60	7503	F/ME	
Grotta dei Ciclami	45.7	13.8	6300±60	7226	F/ME	
Grotta del Cavallo, Trapani, Sicillia	38.0	12.5	5990±80	6833	F/ME	
Grotta del Mitreo, Trieste	45.8	13.6	5770±38	6568	F/ME	
Grotta del Santuario della Madonna, Praia a Mare	40.9	15.8	7555±85	8360	F	TRUE
Grotta del'Orso	44.0	12.9	6080±50	6957	F/ME	
Grotta dell'Edera	45.6	14.9	6500±78	7411	F/ME	
Grotta di Madonna	39.9	15.8	7555±85	8354	F	TRUE
Grotta di Monte Venere	44.3	11.3	6940±100	7782	F/ME	
Grotta di Porto Badisco	40.1	18.5	5850±55	6659	F/ME	
Grotta Pollera	44.1	10.1	6950±10	7796	F	TRUE

Site Name	Latitude	Longitude	DateBP (uncal) ± SD	Average date cal BP (INTCAL09)	Economy	Retained?
			0			
Grotte Bourbon	44.0	4.5	6180±180	7064	ME	
Grotte de Camprafaud	43.4	2.9	6480±130	7382	ME	
Grotte de l'Aigle	44.1	4.6	6138±77	7039	ME	
Grotte de la Baume de Gonvillars	47.6	6.6	5380±250	6166	F	
Grotte de la Vieille Eglise	45.9	6.3	5295±52	6081	F/ME	
Grotte de Puechmargues	44.1	3.2	6420±180	7312	F/ME	
Grotte de Rouffignac	45.3	-0.5	6400±40	7340	un	TRUE
Grotte del'Abbe Pialet	43.9	3.7	6260±90	7163	F/ME	
Grotte du Gardon	46.0	5.3	6325±40	7253	F/ME	TRUE
Grotte du Sanglier	44.7	5.3	6915±70	7758	F/ME	TRUE
Grotte Lombard	43.7	7.9	6150±85	7042	F/ME	
Grotti Aisone, Cuneo	44.3	7.2	5825±75	6631	F/ME	
Grouin du Cou, La Tranche sur Mer	46.4	-1.5	6386±76	7321	ME	TRUE
Gudnja pecina	42.6	18.1	7170±70	8005	F	TRUE
Gufkral	35.9	77.0	3864±115	4284	F	TRUE
Gumelnitsa	44.1	26.3	5715±70	6518	F	
Gundorovka	44.1	26.3	5080±40	5821	un	
Gunnarstorp	59.2	11.1	2970±70	3143	F	
Guzila VI	52.7	18.9	5950±160	6809	F	
Gwernvale	51.9	-2.9	5050±80	5793	F	
Gyalaret	46.2	20.1	7090±100	7905	F	TRUE
Ha Lung	21.1	107.0	6310±60	7243	ME	TRUE
Hacilar	37.6	30.1	7770±180	8653	F	TRUE
Hafir, Algeria	34.8	-2.3	7530±170	8346	un	TRUE
Häggsta I	59.2	17.9	5025±100	5775	F	
Hajji Firuz	37.0	45.5	7269±86	8098	F	
Hakkilan tienhaara	60.3	25.1	6270±50	7191	HG	TRUE
Haldrup Strand	55.9	10.0	5630±120	6439	HG	TRUE
Hallertau	48.6	11.8	5990±90	6842	F	
Hallur	14.3	75.6	3660±105	3990	F	TRUE
Halula	36.4	38.2	7990±40	8863	F	
Harrow Hill	51.9	-2.5	5006±81	5759	F	
Hassi-Mouillah, Algeria	32.1	5.1	5280±250	6053	ME	TRUE

Site Name	Latitude	Longitude	DateBP (uncal) ± SD	Average date cal BP (INTCAL09)	Economy	Retained?
Hassuna	36.1	43.2	7040±200	7882	F	
Hazelton North	51.9	-1.9	4825±49	5544	F	
Hembury	50.7	3.3	5190±87	5966	F	
Hienheim	48.9	11.8	6235±45	7143	F	TRUE
Hjulberga I	59.4	15.1	4830±65	5546	un	
Hodmezovasarhely-Kotacpart	46.4	20.3	6450±100	7358	F	
Hognaston	53.0	-0.3	4930±60	5680	F	
Honeygore Track	51.2	-2.8	4590±40	5283	F	
Il'inka	54.0	51.6	6940±90	7783	HG	
Ile Bono	48.8	-3.6	5195±300	5968	F	
Ile de Geignog	48.6	-3.4	5800±300	6675	ME	
Iliinskaya	53.9	51.1	6940±90	7781	HG	
Ilipinar	40.5	29.3	7111±16	7942	F	TRUE
Imbonga	-0.7	19.8	3775±105	4159	ME	TRUE
Imchin II	51.7	143.0	5810±90	6614	HG	
Imerka 7	54.1	42.9	6270±80	7178	HG	
Inganeset (Kjerringneset IV)	69.2	29.3	5990±55	6834	HG	
Isetskoe Ozero	56.8	60.3	5880±60	6699	HG	
Isl. Surskoi	48.3	35.1	7195±55	8027	ME	
Isle of Riou 1	43.2	5.4	7600±100	8407	ME	
Isola Virginia, Lombardia	45.8	8.7	5534±144	6332	F	
Istok 4			6620±260	7504	un	
Ityrkhei	53.1	106.7	5682±57	6474	HG	
Ivanovka	52.4	53.8	8020±90	8877	HG	
Ivanovskaya	52.5	53.8	8020±90	8878	HG	TRUE
Ivanovskoe 2	52.6	52.2	7080±80	7896	HG	
Ivanovskoe 3	52.6	52.2	7110±80	7931	HG	
Ivanovskoe 7	52.6	52.2	7220±90	8055	HG	TRUE
Iwashita Cave	33.2	129.8	11,300±130	13169	HG	
Iwo Eleru, Nigeria	7.4	5.3	5570±90	6372	un	TRUE
Jangar	47.7	46.0	5890±70	6709	un	TRUE
Jeffs Farm, Lincolnshire	53.1	-0.2	4800±70	5513	F	
Jeitun, Turkmenistan	38.1	58.2	7217±54	8047	F	
Jiangxigou 2	36.7	99.8	7330±50	8129	HG	TRUE
Jyunou	36.2	139.8	11134±124	12996	HG	
Kääpa	57.9	27.1	4712±41	5446	un	
Kairshak 1	46.8	48.3	7230±90	8063	HG	

Site Name	Latitude	Longitude	DateBP (uncal) ± SD	Average date cal BP (INTCAL09)	Economy	Retained?
Kairshak 3	46.8	48.3	7950±90	8811	HG	TRUE
Kalavassos-Tenta	34.8	33.3	5830±60	6630	F	TRUE
Kalibangan	29.4	74.1	4195±115	4726	F	TRUE
Kalmozero 11	64.1	32.5	6340±70	7269	HG	TRUE
Kalvebeitiet (Site 27)	61.2	7.8	2250±70	2247	HG	
Kamabai	9.2	-12.0	2560±115	2612	F/ME	TRUE
Kamenna Mogila	47.2	35.4	7250±95	8077	ME	TRUE
Kamikuroiwa	33.7	133.0	12165±600	14591	HG	TRUE
Kanispur	34.2	74.4	4490±100	5140	F	TRUE
Kara-Tenesh	51.0	86.3	5440±60	6228	HG	TRUE
Karavaikha 4	60.4	38.8	6930±50	7763	HG	TRUE
Kashkashok II	36.7	40.6	7880±110	8741	F	TRUE
Kaster	50.8	3.5	5853±42	6665	F	TRUE
Katalszeg	46.1	21.1	6370±100	7291	F	
Kayukovo 2	60.2	72.8	6810±40	7644	HG	TRUE
Keio SFC	34.5	139.5	11350±160	13219	HG	TRUE
Kercado	47.6	3.1	5840±300	6689	un	
Khairadih	26.2	81.9	3990±100	4477	F	
Khant de Saint-Louis, Senegal	16.5	-16.1	5650±40	6427	HG	TRUE
Khummi	50.6	137.1	13260±100	16168	HG	TRUE
Khvalynsk II	52.5	48.1	6200±85	7091	ME	TRUE
King Barrow Ridge (Stonehenge Environs)	51.2	-1.8	4578±94	5241	F	
Kintampo K1	8.1	-1.7	3560±100	3857	ME	
Kintampo K6	8.0	-1.7	6100±250	6979	un	TRUE
Kintampo K8	8.1	-1.7	3570±84	3870	ME	
Kirchnaumen-Evendorff	45.4	6.6	6050±200	6914	F	
Kitoi Yarki	52.6	104.1	7990±350	8915	HG	TRUE
Klein Denkte	52.1	10.6	6050±110	6927	F	
Kmehlen	51.4	13.7	5360±160	6132	F	
Knockiveagh, Co Down	54.3	-5.8	5020±170	5783	F	

Site Name	Latitude	Longitude	DateBP (uncal) ± SD	Average date cal BP (INTCAL09)	Economy	Retained?
Knossos	35.5	25.2	7000±180	7849	F	TRUE
Kodekal	16.35	76.4	4285±105	4865	un	TRUE
Koksharovskij Holm	58.3	60.7	5960±81	6804	HG	TRUE
Köln-Mengenich	50.9	7.0	6320±70	7245	F	
Konens Høj	56.0	10.7	5260±100	6051	ME	
Konispol Cave	39.7	20.2	7545±76	8344	F	
Konjonjoki	60.7	22.7	5790±140	6605	HG	
Kõpu I	58.9	22.3	5698±70	6498	HG	TRUE
Korchugan 1a	56.5	76.3	6740±100	7601	HG	TRUE
Korlat	48.4	21.3	6440±100	7353	F	TRUE
Kornachak II	53.8	84.9	7340±175	8165	HG	TRUE
Kosan-ni	33.3	126.2	10180±65	11852	HG	TRUE
Koshinskaya	57.6	48.2	8350±100	9324	HG	TRUE
Kovacevo	41.4	23.0	7180±45	8002	F	
Krasnostavka	49.1	30.4	5310±160	6084	F	
Krasnoye Selo	53.2	24.5	5052±25	5818	un	
Krasnyj Gorodok	53.8	50.8	6730±100	7594	HG	
Krasnyj Yar	53.6	50.7	6540±80	7449	HG	
Kraviojankangas	61.2	22.3	6060±170	6931	HG	TRUE
Kubodera-Minami	36.9	138.5	12630±50	14912	HG	
Kudrukula	59.5	28.1	4815±42	5533	HG	
Kukhtui	59.4	143.2	4700±100	5410	HG	TRUE
Kumartepe	37.5	38.5	7930±80	8798	F	TRUE
Kunjhun	24.6	82.2	4740±80	5459	F	TRUE
Kurkijokki	60.2	29.9	7900±80	8768	HG	TRUE
Kuznetsovo III	46.1	141.9	5865±99	6679	HG	TRUE
Kuzuharasawa IV	35.1	138.5	11400±140	13267	HG	
La Croix Maigret	47.9	1.1	6030±130	6906	F/ME	TRUE
La Cueva del Nacimiento	38.1	-1.7	6780±130	7645	F/ME	TRUE
La Dehesilla	36.7	-5.6	7127±123	7951	ME	TRUE

Site Name	Latitude	Longitude	DateBP (uncal) ± SD	Average date cal BP (INTCAL09)	Economy	Retained?
La Draga	42.1	2.8	6700±710	7657	ME	TRUE
La Falguera Rock shelter	43.1	-6.2	6510±70	7414	ME	TRUE
La Fosse Toumise	49.4	3.4	5870±105	6684	F	
La Hoguette	49.1	0.4	5560±150	6348	un	
La Pietra	42.6	8.9	5945±160	6793	ME	
Laang-Spean	12.9	102.9	6240±70	7143	HG	TRUE
Lambourn	51.5	-1.5	5365±180	6137	F	TRUE
Lamersdorf	50.8	6.5	6410±45	7345	F	
Langweiler II	50.8	6.4	7080±65	7901	F	TRUE
Lanino II	57.2	33.0	6440±370	7323	HG	
Latokangas	65.1	26.2	5795±90	6596	HG	
Lautereck/ Felsdach Lauterach	48.3	9.6	6140±45	7045	F	
Le Coq Galleux	49.4	2.8	6080±110	6962	F	TRUE
Le Guerzit II	48.7	-3.8	5950±110	6803	F/ME	TRUE
Le Moulin	44.2	5.5	5840±130	6661	ME	
Le Roc de Dourgne	42.6	2.2	6170±100	7059	ME	
Le Trou du Diable	47.3	4.8	5105±55	5832	un	
Lebyazhinka 4	53.8	50.9	6680±80	7552	HG	
Lelystad	52.5	5.5	5540±65	6346	HG	
Lengbe	1.7	28.6	850±70	3113	F	TRUE
Lepinski Vir	44.5	22.0	7300±124	8136	HG	
Les Coudoumines	42.8	2.6	5135±36	5863	ME	
Les Dependances de Digny	48.2	2.4	5987±41	6825	F	
Les Gouillauds	45.5	-0.6	5950±120	6803	ME	
Les Grands Traquiers	49.0	4.3	6200±140	7081	F	TRUE
Les Longrais	47.5	7.2	5210±102	5987	ME	
Les Reaudins	48.4	3.2	5800±50	6600	un	
Les Rivaux	45.1	3.9	6240±110	7137	un	
Leushi 9	59.3	65.8	7590±80	8393	HG	TRUE
Leushi VII	59.6	65.7	6890±70	7735	HG	
Lietzow-Buddelin II	54.5	13.5	5815±100	6621	HG	TRUE
Liffs Low	53.1	-1.8	5270±70	6060	F	TRUE

Site Name	Latitude	Longitude	DateBP (uncal) ± SD	Average date cal BP (INTCAL09)	Economy	Retained?
Limonesque	44.4	3.5	5510±200	6307	ME	
Linlithgow	56.0	-3.6	5865±55	6676	F	TRUE
Lipetskoe Ozero	52.6	39.6	5310±110	6099	HG	
Little Hoyle Cave, Pembrokeshire	51.7	-4.7	4847±47	5574	F	
Little Waltham	51.8	0.5	5120±130	5880	F	TRUE
Littleour	56.6	-3.4	4600±50	5304	F	
Llandegal	53.2	-4.1	5240±150	6016	F	
Lochhill	57.7	-3.2	5070±150	5839	F	TRUE
Lojewo	52.7	18.3	6180±100	7074	F	
Lokalitet Tumba	41.0	21.8	6760±110	7625	F	
Lokomotiv	52.3	104.3	6670±70	7543	HG	
Lonelega I	59.2	6.9	2780±110	2923	un	
Long Down (Flint Mine), West Sussex	50.9	-0.7	4975±71	5725	F	
Lopé 12	-0.2	11.6	2280±80	2289	F	
Lopé 2	-0.2	11.6	2370±35	2412	F	
Lossoa's hus	70.1	28.9	6315±90	7232	HG	
Lothagam Hill ZU-4, Kenya	2.0	36.0	8420±170	9399	HG	TRUE
Lough Derravaragh	53.6	-7.4	5360±110	6134	F	
Lower Luggy, Powys	52.6	-3.2	4830±45	5549	F	
Lugovoe	54.1	48.3	6700±100	7573	HG	
Luka Vrublivetska	48.6	26.7	5870±38	6695	F	
Machrie Moor, Arran	55.5	-5.3	4808±44	5527	F	
Mad Man's Window, Glenarm, Antrim	55.0	-5.9	5095±120	5845	F	
Maddalena di Muccia	43.1	13.1	6580±75	7483	F	
Maes Howe	59.0	-3.2	5094±60	5829	F	TRUE
Maiaki	46.4	30.3	4412±29	4990	F	TRUE
Maiden Castle, Dorset	50.7	-1.5	4811±36	5532	F	
Majdanetskoe	48.8	30.5	4890±50	5629	F	
Maksimovka 1	53.0	51.7	6470±80	7378	HG	
Makubasi NW	1.8	29.0	971±33	3033	ME	
Maltan	62.2	150.6	4450±110	5099	HG	TRUE
Maluba	2.8	18.5	2140±200	2147	ME	TRUE
Marawah 1	24.3	53.3	7036±30	7881	F	TRUE

Site Name	Latitude	Longitude	DateBP (uncal) ± SD	Average date cal BP (INTCAL09)	Economy	Retained?
Marevka	48.4	35.3	7955±55	8820	HG	TRUE
Margineda Cave	42.2	1.6	6740±94	7605	ME	
Masseria Candelaro	41.6	15.9	6200±95	7098	F	
Masseria Giuffreda	41.4	15.6	7125±20	7954	F	
Matarrah	35.2	44.4	7570±250	8424	F	TRUE
Matveev Kurgan I	47.6	38.9	7239±63	8068	ME	TRUE
Meare Heath Field	51.2	-2.8	5180±70	5944	F	TRUE
Medulin-Vizula	44.8	13.9	6850±180	7727	F	TRUE
Mehrgarh	29.4	67.6	4530±70	5175	F	TRUE
Meindling	48.8	12.6	6123±31	7026	F	
Menneville	49.4	4.0	6030±130	6899	F	
Mennikka (Skogfoss)	69.4	29.7	5975±60	6811	HG	
Mersin (Yumuktepe)	36.8	34.6	7545±75	8340	F	TRUE
Messum 1	-21.4	14.3	1370±50	2615	F	TRUE
Midgeholme Moss	54.9	-2.6	5270±90	6060	F	TRUE
Midtown of Pitglassie	57.5	-2.5	4935±105	5690	F	
Mileto	43.8	11.2	6180±80	7081	F	
Millbarrow	51.5	-1.9	4900±110	5657	F	
Miyagase Kitahara	35.5	139.2	13047±37	15745	HG	
Mohelnice	49.8	16.9	6345±71	7278	F	
Molebnoe ozero 1	55.0	46.6	6290±90	7192	HG	
Molino Casarotto VI	45.5	11.6	5960±50	6796	F	
Monamore	55.5	-5.1	5110±110	5861	F	
Monte Leone	41.4	9.2	5855±95	6664	F	
Monte Maulo	41.6	14.6	6540±80	7440	F	
Monte Rocca, Rivoli	45.5	11.6	5670±130	6485	F	
Mossby	55.4	13.6	6480±70	7383	F	TRUE
Mumute	8.7	-1.7	3350±100	3611	ME	
Munhata	32.6	35.6	7370±400	8279	F	
Nabta (E-77-7), Egypt	22.5	30.7	8960±110	10028	HG	
Nakajima B	36.2	138.1	12460±310	14695	HG	
Nanzhuangtou	39.0	115.7	10509±140	12353	HG	TRUE
Narva Joaoru	59.4	28.2	5820±200	6659	HG	

Site Name	Latitude	Longitude	DateBP (uncal) ± SD	Average date cal BP (INTCAL09)	Economy	Retained?
Navolok	66.5	40.6	4840±70	5560	HG	TRUE
Ndjolé Pk5	0.2	10.8	2370±55	2455	un	
Nea Nikomedeia	40.6	22.3	8180±150	9123	F	TRUE
Neckenmarkt	47.6	16.5	6142±42	7049	F	
Nellimöjoen suu S	68.8	28.3	6000±120	6866	HG	
Nerpich'ya Guba I	68.4	38.4	4630±100	5328	HG	
Neuburg/Poel XII	54.0	11.5	5621±29	6390	HG	
Newton, Islay	55.8	-6.2	4965±60	5712	F	
Niedermerz	50.9	6.3	6800±80	7655	F	
Niemcza	54.0	14.8	6210±80	7106	F	TRUE
Nikol'skaya pravaya	55.9	36.5	6470±70	7378	HG	TRUE
Nikolskoye Cemetary	48.4	35.2	6202±52	7098	ME	
Nizhnetytkes-ken	53.1	85.5	5440±105	6207	HG	
Nizhnyaya Dzhilinda I	55.5	115.9	7880±80	8740	HG	TRUE
Noatun Innmarken	69.2	29.3	6185±65	7084	HG	TRUE
Nordli	70.1	28.5	6570±60	7480	HG	TRUE
Norrois	48.7	4.6	6020±110	6890	F	
North Mains, Strathallen	56.3	-3.7	4640±65	5370	F	
Northeim-Imbshausen	51.8	10.1	6192±140	7079	F	
Nottuln	51.9	7.4	5585±45	6366	F	TRUE
Novopetrovka II	49.6	128.4	12720±130	15070	HG	TRUE
Novorozanovka II	48.1	31.1	4904±300	5619	F	
Nowodworce I	53.3	23.4	6000±150	6873	HG	TRUE
Ntereso	9.1	-1.2	3580±130	3895	ME	
Nymolla III	56.0	14.5	5930±60	6765	ME	
Oblon	46.3	32.2	4630±40	5384	F	TRUE
Obre I	44.2	18.1	7240±60	8069	F	TRUE
Odai Yamamoto I	41.2	140.5	13780±170	16899	HG	TRUE
Odmut	45.2	18.8	6970±71	7807	F	
Offham Hill	50.9	0.0	4925±80	5677	F	
Okanda I	-0.1	11.6	3560±75	3851	un	TRUE
Okopi	51.5	29.6	6330±65	7259	F	TRUE
Ølby Lyng	55.5	12.2	5265±92	6053	HG	
Old Yelshanskay II	52.3	53.1	6820±80	7673	HG	
Oleye-Al Zèpe	50.7	5.2	6307±32	7229	F	
Olszanice	50.1	19.8	6415±41	7348	F	TRUE

Site Name	Latitude	Longitude	DateBP (uncal) ± SD	Average date cal BP (INTCAL09)	Economy	Retained?
Opatowice 33	52.7	18.6	6190±120	7078	ME	
Opukha, Bering Sea Coast	61.8	174.1	2600±100	2651	HG	TRUE
Orunsumo, Aohan Banner (Chifeng)	43.5	118.7	8040±80	8903	un	TRUE
Osan-ni	38.2	128.6	7120±700	8172	HG	TRUE
Osimenki 2	53.8	44.0	6950±170	7793	HG	TRUE
Osipovska Cemetary	49.9	30.4	7955±55	8818	HG	TRUE
Osovets IV	54.9	29.5	5860±50	6676	HG	TRUE
Ostoros	47.9	20.4	6180±100	7067	F	
Östra Jansmyra I	60.3	20.1	6084±55	6963	HG	TRUE
Östra Vrå	60.3	20.1	5015±50	5771	HG	
Oszentivan VIII	46.2	20.2	6460±80	7370	F	
Otoumbi 13	-0.1	11.1	2390±65	2485	un	
Oursi	14.7	-0.5	2931±32	3091	F	
Padrão	37.1	-8.9	6849±38	7680	ME	
Pahkakoski	65.4	26.0	5713±55	6509	HG	
Paiyampali	12.6	78.4	3435±100	3704	F	TRUE
Panozero 1	63.3	33.3	5795±35	6593	HG	
Parow	54.4	13.1	5136±23	5887	F	
Parta	45.6	21.2	6777±32	7626	F	
Passy	48.1	3.3	6065±55	6929	F	
Peak Camp (Cowley)	51.8	-2.2	4840±71	5560	F	
Pechora	48.8	28.7	7288±40	8096	HG	TRUE
Pegrema IX	62.6	34.4	6510±90	7410	HG	TRUE
Pen-y-Wyrlod	52.0	-3.2	4970±80	5733	F	
Pena d'Água Rock-shelter	39.6	-8.6	6775±60	7626	ME	
Pendimoum	43.8	7.5	6390±100	7304	ME	
Pengdoushang	29.7	111.6	8300±80	9284	HG	TRUE
Penne Di Pescara	42.5	13.9	6578±135	7467	F	
Pereval	42.9	133.1	8380±60	9387	HG	TRUE
Petit Mont	47.5	-2.9	5600±70	6391	F	
Petriolo III South	43.2	13.5	7480±100	8279	F	TRUE
Petrovska balka	45.3	34.2	4670±80	5396	F	TRUE
Pezmog 4	61.8	52.2	6820±70	7665	HG	TRUE
Pfyn	47.6	8.9	4993±20	5714	F	
Piana di Curinga	38.8	16.3	6930±60	7766	F	TRUE
Piestinya/Piestene	57.9	27.5	4670±150	5352	F	
Pizzo di Bodio	45.8	8.8	6320±80	7241	F	TRUE

Site Name	Latitude	Longitude	DateBP (uncal) ± SD	Average date cal BP (INTCAL09)	Economy	Retained?
Planta	46.2	7.4	6500±80	7406	F	TRUE
Plussulien	48.2	-3.0	5210±99	5987	F	
Poggio Vento, Agrigento, Sicily	37.3	13.6	6130±90	7016	F	
Poigen	48.7	15.6	5935±90	6772	F	
Pokrovnik I	43.8	16.0	7000±100	7825	F	
Polivaniv Yar	48.1	26.8	5440±70	6218	F	
Pontcharaud	45.8	3.1	7095±50	7914	F	TRUE
Portiragnes	43.3	3.3	6435±135	7337	F	
Povenchanka XV	63.1	35.3	4270±60	4820	HG	
Prilukskaya	61.3	42.4	6680±70	7548	HG	TRUE
Pristina	42.7	21.2	6280±80	7187	F	TRUE
Protoka	56.5	76.4	6355±200	7219	HG	
Pugach II	47.9	31.2	6895±50	7730	ME	
Pundo	0.0	34.0	7000±40	7842	HG	
Pupicina Cave	45.3	14.2	6590±240	7460	F	
Putineshti	47.8	28.1	5595±80	6396	F	
Puzi II	51.2	142.7	8780±135	9869	HG	TRUE
Pyalitsa XVIII	66.2	39.8	4700±70	5436	HG	
Pyasina I	70.9	89.6	4960±50	5700	HG	TRUE
Raigmore, Inverness	57.5	-3.8	4813±74	5528	F	
Rakushechny Yar	47.6	40.7	7806±72	8614	HG/ME	TRUE
Ralswiek-Augustenof	54.5	13.5	5471±41	6266	HG	
Ras Shamra	35.6	35.8	7686±112	8508	HG	TRUE
Ravin de la Mouche	14.3	-3.5	9785±70	11194	HG	TRUE
Rectory Farm	52.3	-0.2	4950±36	5676	F	
Redlands Farm	52.3	-0.6	4823±50	5540	F	
Rehmsdorf	51.0	12.1	5993±79	6845	F	TRUE
Reichstett	48.6	7.8	5940±140	6787	F	
Renaghju	41.5	8.9	6525±60	7431	ME	
Rendina	41.0	16.0	6891±81	7740	F	
Revellata	42.6	8.7	6280±75	7193	un	
Rhum	57.0	-6.3	4725±140	5420	ME	TRUE
Ricoh	48.1	7.3	6400±70	7326	F	
Riigiküla IV	59.4	28.1	6023±95	6886	HG	TRUE
Ringkloster	56.0	10.0	5555±78	6358	HG	
Ripa Tetta, Lucera	41.5	15.3	6890±60	7735	un	
Riparo Arma di Nasino	44.1	8.1	5980±85	6833	F	

Site Name	Latitude	Longitude	DateBP (uncal) ± SD	Average date cal BP (INTCAL09)	Economy	Retained?
Riparo del Lauro di Candalla II	43.9	10.3	5250±40	6031	F	
Riparo di Romagnano III	46.0	11.1	6480±50	7382	F	TRUE
Riparo Gaban	46.1	11.1	6030±45	6873	F	
Rivaltella-Ca'Romensini	44.7	10.6	6070±110	6949	F	
Riviere Denis I	0.3	9.3	4810±80	5523	un	
Robin Hood's Ball (Stonehenge Environs)	51.2	-1.9	4613±67	5315	F	
Rochas	44.4	4.5	6090±210	6962	ME	
Rockmarshall Midden	54.0	-6.3	5470±110	6245	F	TRUE
Rocquemissou VIIIc1	44.4	2.7	7151±166	7988	ME	TRUE
Rodingen	51.0	6.6	6250±75	7151	F	
Rognlien	59.1	9.8	4600±130	5270	un	TRUE
Rogozhany	47.8	28.4	5700±55	6496	F	
Roinila	64.9	29.0	5975±105	6826	HG	TRUE
Roquefort	44.0	3.0	5680±200	6500	F	
Rosdorf Niedersachsen	51.5	9.9	6350±70	7284	F	
Rosenburg	48.6	15.7	6650±60	7526	F	
Rosenhof	54.3	11.1	5960±65	6799	HG	
Rotten Bottom	55.4	-3.4	5040±100	5784	F	
Roucadour	44.8	1.5	5940±150	6794	F	TRUE
Route de Rouffach	48.1	7.3	6062±81	6934	F	
Rowden, Winterbourne Steepleton	50.7	-2.6	5250±140	6034	F	TRUE
Rudnaya Pristan	44.4	135.8	7561±43	8372	HG	TRUE
Rudnya Serteiskaya	56.3	31.5	6240±40	7157	HG	
Rufacher Huben	48.0	7.3	5832±74	6642	F	
Rugland, Jaeren	58.6	5.7	3550±115	3857	ME	TRUE
Ruhnu II	57.8	23.3	5400±83	6165	un	TRUE
Rusavierto	62.7	25.2	5985±80	6837	HG	TRUE
Ruseshti	46.9	28.8	5565±100	6366	F	TRUE
Sabatinovka II	48.2	30.2	6089±41	6967	F	
Sablieres de Libreville	0.5	9.4	5710±80	6508	HG	TRUE
Sadovniki II	47.2	142.1	6612±134	7501	HG	TRUE
Safiet Bou Rhenan, Algeria	34.4	3.5	6970±170	7819	F	

Site Name	Latitude	Longitude	DateBP (uncal) ± SD	Average date cal BP (INTCAL09)	Economy	Retained?
Sagan-Zaba	53.1	106.2	7630±45	8435	HG	
Saggai, Sudan	15.9	32.6	10060±150	11670	HG	TRUE
Saint Just	47.8	-2.0	5770±80	6576	un	TRUE
Sakhtysh 2a	56.8	40.4	7356±30	8163	HG	TRUE
Salasun	-1.5	36.8	7255±225	8085	un	TRUE
Saliagos	37.1	25.1	6172±74	7066	F	TRUE
Salpetermosen	55.9	12.3	6020±100	6889	HG	TRUE
Sammardenchia	45.7	13.8	6570±74	7475	F	TRUE
Samsonovskoe	47.7	20.2	7460±200	8277	HG	TRUE
San Marco, Gubbio	43.1	12.4	6430±80	7350	F	
Sang-I-Chakmak	36.4	55.1	7476±100	8280	F	TRUE
Sanganakallu	15.2	77.0	3540±100	3832	F	
Sangnodae Do	33.7	128.6	6430±180	7311	HG	
Santa Tecchia	41.5	15.7	6520±70	7429	F	
Sanyasula Gavi	15.5	78.2	3515±35	3784	F	
Sarn-y-Bryn-Calod	52.6	-3.2	4960±70	5714	F	
Sarnate	57.1	21.4	4648±93	5356	HG	TRUE
Sartinya I	64.2	65.5	6535±57	7444	HG	TRUE
Sarurab, Sudan	15.9	32.5	9355±78	10570	HG	
Savignano sul Panaro	44.5	11.0	5930±130	6770	F	
Savran’	48.1	30.0	6985±60	7821	ME	
Scamuso	41.1	16.9	7290±110	8116	ME	
Schamli	48.6	7.8	6618±172	7499	F	TRUE
Schenkon	47.2	8.1	4980±120	5742	F	
Schlamersdorf	53.9	10.3	6385±60	7322	HG	TRUE
Schwanfeld	43.9	10.1	7900±80	8763	F	TRUE
Schwindratzeim	48.8	7.6	6230±300	7100	F	
Seamer Moor	54.3	-0.5	5030±90	5779	F	TRUE
Seedorf	54.0	10.5	5935±65	6771	HG	
Seiko Sanso B	36.8	138.2	12340±50	14387	HG	
Selevac	44.5	21.9	6192±51	7090	F	
Semenovka	49.8	33.5	7058±44	7890	ME	TRUE
Sente Saillancourt	49.1	2.0	5220±110	6004	F	

Site Name	Latitude	Longitude	DateBP (uncal) ± SD	Average date cal BP (INTCAL09)	Economy	Retained?
Sepulchral Cave, Derbyshire	53.3	-1.2	4750±64	5472	F	
Sergeevka	50.8	127.3	7940±45	8809	HG	TRUE
Serteya X	56.3	31.5	7342±164	8172	HG	TRUE
Servia-Varytimides	40.2	22.0	6905±87	7755	F	
Sesklo	39.4	22.8	7525±16	8361	F	TRUE
Seuil des Chèvres	45.7	5.4	6320±260	7186	F	
Sha'ar Hagolan	32.7	35.6	7495±50	8304	F	TRUE
Shajdurikhinskoe 5	57.3	60.6	5910±90	6746	HG	
Shcherbet 2	55.0	49.5	6620±90	7512	HG	TRUE
Shelter Jean Cros	43.1	2.5	6584±119	7473	F	TRUE
Sheltozero 11	61.4	35.4	6480±70	7387	HG	
Shippea Hill	52.4	0.4	4910±85	5661	F	
Shirokaya Balka	46.6	32.2	4250±60	4783	F	
Shkarovka	49.7	30.2	5015±105	5771	F	
Shomu-Tepe, Azerbaijan	39.9	47.5	7510±70	8311	F	TRUE
Shulaver I, Marneuli	41.5	44.8	6625±210	7511	F	
Shum Laka	5.9	10.1	7140±50	7959	HG	TRUE
Shurton Hill	50.9	-0.6	4750±50	5481	F	
Sidari	39.8	19.7	7568±100	8370	F	TRUE
Sikazegashira	31.4	130.2	11820±35	13664	HG	TRUE
Siktyakh I	70.0	125.0	5220±170	5997	HG	TRUE
Silino	60.6	29.6	5830±80	6634	HG	
Silvola	60.3	24.9	5950±50	6783	HG	
Sion-Petit Chasseur	46.2	7.4	5110±57	5843	F	
Siphiso Shelter	-26.2	32.0	1970±390	2000	HG	TRUE
Siror, GpJb 16	0.2	34.3	7735±35	8509	HG	TRUE
Site 12, Dundrum Nature Reserve, Co Down	54.3	-5.8	4666±97	5369	F	
Site Launey	23.3	5.8	8475±100	9452	un	TRUE
Skara Brae	59.1	-2.7	4406±55	5031	ME	
Skarin Samograd	43.5	16.1	6745±37	7608	F	
Skrivarhelleren	61.2	7.7	3610±50	3924	F	TRUE
Slavonski Brod–Galovo 2	45.2	18.0	6830±110	7690	F	
Smällan II	59.2	17.8	5090±51	5825	un	
Sofievka	49.6	31.3	4300±35	4874	F	
Sokol’tsy II	48.2	30.2	7435±41	8265	ME	TRUE

Site Name	Latitude	Longitude	DateBP (uncal) ± SD	Average date cal BP (INTCAL09)	Economy	Retained?
Sølager	55.9	11.9	5520±110	6315	HG	
Sopka 2/3	55.6	76.8	6285±90	7187	HG	
Soroki II	48.2	28.3	6830±150	7704	ME	
Soroki-Ozero	48.2	28.3	4866±74	5599	ME	
Soulac-sur-Mer (La Balise)	45.5	-1.1	5910±150	6755	un	
Soumont-Saint-Quentin (La Brèche au Diable)	48.7	-0.2	5140±140	5917	un	
Source de Reselauze	43.5	3.3	6450±100	7366	ME	
Spong Hill	52.7	-2.4	4990±80	5743	F	
St. Anna III	40.5	17.6	6780±90	7641	F	
Stanovoe IV	56.9	39.0	6650±160	7533	un	
Staraya Elshanka 2	52.4	53.1	6820±80	7673	HG	
Starodubskoye III	47.4	142.8	6465±85	7372	HG	
Strachow 2	50.9	16.8	6146±34	7056	F	TRUE
Street House Farm, Loftus	54.6	-0.8	4975±28	5699	F	
Strette	42.7	9.2	6460±246	7327	ME	
Stretto, Partanna	38.1	13.4	6630±120	7513	F	TRUE
Stril’chaia skelia	48.0	35.2	5365±70	6142	ME	
Strögen	48.7	15.1	6365±99	7285	F	
Strzelce	53.3	18.1	6260±60	7160	F	
Studenoye I	50.2	108.5	11000±90	12881	HG	TRUE
Sturovo	47.8	18.7	6215±71	7113	F	TRUE
Stuttgart-Bad-Cannstatt	48.8	9.2	6353±45	7291	F	
Suberde	37.4	31.9	7957±58	8817	F	
Sukhaya Vodla II	62.4	37.1	4810±60	5522	HG	
Sulgu 2	62.0	33.2	6085±30	6954	HG	
Sulka	56.8	27.0	4850±60	5574	un	TRUE
Sumpan'ya VI	59.5	67.7	9920±80	11418	HG	TRUE
Sumpanya 4	59.8	64.9	6850±60	7689	HG	
Sventoji IV	56.0	21.1	5110±110	5862	ME	TRUE
Sweet Track	51.2	-1.2	5134±27	5875	F	
Swifterbant 11	52.6	5.6	6308±32	7227	HG	
Szamossalyi	51.5	14.1	6136±100	7023	F	
Szarvas No.23	46.9	20.5	6620±60	7513	F	
T. Narsipur	12.2	76.9	3755±110	4136	F	TRUE
Tabaqat al-Bûma	32.5	35.7	7350±16	8172	F	

Site Name	Latitude	Longitude	DateBP (uncal) ± SD	Average date cal BP (INTCAL 09)	Economy	Retained?
			0			
Tabuyaobao	43.5	118.7	5679±104	6485	un	
Tagalagal	17.8	8.8	9370±128	10634	HG	TRUE
Tainiaro	65.7	25.1	5892±59	6718	HG	
Tall-i-Bakun B	30.0	52.8	6264±70	7171	F	TRUE
Tamsagbulag 1	47.2	117.3	5590±120	6392	HG	TRUE
Tankardstown Site 4/2, Co Limerick	52.4	-7.4	4865±57	5602	F	
Tankardstown, Limerick	52.4	-8.6	5029±22	5805	F	TRUE
Tarnabod	47.7	20.2	6280±100	7185	F	
Tekkalakota	15.5	76.9	3625±100	3947	F	
Tell Arpachiyah	36.3	43.2	8064±78	8944	F	TRUE
Tell Azmak	42.5	25.8	7303±150	8129	HG	TRUE
Tell Halaf	36.8	40.0	7570±35	8381	F	
Tell Karanovo	42.5	25.9	6690±71	7557	F	
Tell Kashkashok	36.6	40.7	7880±110	8737	F	
Tell Nebi	34.5	36.5	8010±35	8879	F	TRUE
Tell Sabi Abyad	36.5	39.1	8040±35	8914	F	TRUE
Tell Seker al-Aheimar	37.9	42.2	7900±160	8769	F	TRUE
Tell Shimshara	36.3	45.0	7940±150	8814	F	TRUE
Tell-es-Siwwan	34.4	43.8	7456±73	8268	F	TRUE
Telul-eth-Thalathat	36.4	42.8	7714±67	8497	F	
Tenteksor	47.0	48.1	6640±80	7520	HG	
Tenteksor 3	47.0	48.1	7005±90	7830	HG	
Tenteksor I	47.0	48.1	7235±45	8063	HG	
Tepe Gawra	36.6	43.3	7002±82	7831	F	
Tepe Gaz Tavileh (Yahya)	28.3	56.6	6650±180	7534	F	TRUE
Tepe Guran	33.6	47.1	7760±150	8619	F	
Tepe Sabz	32.5	47.4	7454±158	8258	F	
Tepe Sarab	34.1	47.3	7956±98	8815	F	TRUE
Terkuemkyun, Eastern Chukotka	65.2	173.8	4580±40	5250	HG	TRUE
Terres de Prepoux II	48.3	3.1	6730±110	7596	F	TRUE
Thalathat II	36.6	42.5	7620±50	8429	F	
The Ord North	58.0	-4.4	4614±57	5330	un	
The Trundle, West Sussex	51.8	0.5	4860±10	5590	F	

Site Name	Latitude	Longitude	DateBP (uncal) ± SD	Average date cal BP (INTCAL09)	Economy	Retained?
			0			
Theopetra Cave	39.7	21.7	8046±27	8941	F	TRUE
Thielle-Mottaz	47.0	7.0	5280±110	6067	F	
Thirlings, Northumberland	55.6	-2.1	5230±150	6011	F	
Ti-n-Akof	15.0	-0.2	3479±45	3751	HG	
Ti-n-Hanakaten (Algeria)	23.9	10.4	8100±130	9012	HG	
Ti-n-Torha Two Caves (Libya)	25.0	10.3	8840±60	9928	HG	
Til'kin, Turkmenistan	38.1	57.8	6590±110	7480	F	
Timidouin, Algeria	24.3	5.6	8100±130	9016	HG	TRUE
Timokovo	48.0	29.0	5700±70	6504	F	
Tinj I	44.0	15.5	6895±136	7751	F	
Tintane pécheur, Mauritania	20.9	-15.3	6193±109	7090	F	TRUE
Tiszavasvari-Keresztfal	48.0	21.4	6226±69	7127	F	
Togolok-Depe, Turkmenistan	38.1	58.0	7320±100	8139	F	TRUE
Tokarevo I	60.5	28.8	4790±210	5477	HG	
Tokumaru Nakata	36.3	139.2	13700±560	16546	HG	TRUE
Tongsamdong	35.1	129.1	5900±99	6727	HG	TRUE
Torihama	35.6	135.9	11830±55	13668	HG	TRUE
Townhead, Rothesay, Bute	55.8	-5.1	4070±100	4586	F	
Toyretepe	41.0	45.0	6085±120	6965	F	
Tsaga I	67.7	35.1	5760±160	6588	HG	TRUE
Tuba Ajuz I	12.1	13.2	3150±38	3378	ME	
Tudozero 5	61.2	36.4	6600±25	7494	HG	TRUE
Tudozero V	61.2	36.4	6250±50	7165	HG	
Tully, Aldergrove Airport	54.5	-7.8	4960±85	5718	F	
Tutkaul, Tadjikistan	38.0	69.2	7100±140	7933	un	TRUE
Twann	47.1	7.2	5019±34	5783	F	
Tyniec Maly	51.0	16.9	5223±60	6011	un	
Tyttinge	59.2	17.8	5815±75	6617	HG	TRUE
Uan Afuda (Libya)	24.6	10.6	8935±100	10016	HG	TRUE
Uan Tabu	25.0	11.0	8880±100	9954	HG	

Site Name	Latitude	Longitude	DateBP (uncal) ± SD	Average date cal BP (INTCAL09)	Economy	Retained?
Ulan-Khada	53.2	107.0	7650±80	8456	HG	TRUE
Ulm-Eggingen	48.4	9.9	6500±100	7403	F	TRUE
Unang	44.1	5.2	5950±130	6803	ME	
Uniondale Rock Shelter	-33.3	26.5	2152±55	2163	HG	TRUE
Universitetskaya III	51.7	39.2	5080±125	5831	ME	
Unoki-Minami	36.5	138.0	11630±50	13480	HG	
Unterpullendorf	47.5	16.5	6004±81	6852	F	
Urutlekrai (Site 47)	61.2	7.7	2438±22	2497	HG	
Usatovo	46.5	32.7	4330±60	4931	F	
Ust'-Drozdovka	68.3	38.5	5510±100	6305	HG	TRUE
Ust'-Karenga	54.5	116.5	12180±60	14040	HG	TRUE
Ust'-Kazachka	55.7	95.1	6660±190	7545	HG	TRUE
Ust'-Khaita	52.9	103.2	7245±150	8078	HG	
Ust'-Khemchik	51.7	91.8	6500±110	7409	HG	TRUE
Ust'-Kiakhta	50.5	106.2	12595±50	14841	HG	TRUE
Ust'-Kova	58.6	100.6	6195±70	7088	HG	TRUE
Ust'-Menza I	50.3	108.5	8715±60	9698	HG	
Ust'-Tashelka	53.9	48.1	7810±190	8692	HG	TRUE
Ust’-Rybezhnoye	60.4	32.6	6380±220	7246	HG	TRUE
Utajärvi (Pyhänniska)	64.8	26.4	6140±105	7027	HG	
Utnur	16.0	77.6	3933±69	4368	un	TRUE
Utyuzh 1	55.1	46.6	6330±90	7249	HG	TRUE
V'yun	60.6	32.6	5980±100	6838	HG	
Vailly-sur-Aisne	49.5	3.5	5470±300	6284	ME	
Vallon-des-Vaux	43.8	6.8	4985±35	5721	F	
Varasti	44.2	27.0	5360±70	6137	F	
Varfolomeevskaya 2B	50.7	47.7	7070±80	7886	HG	TRUE
Varga 2	57.4	60.1	7106±35	7932	HG	TRUE
Vargstensslätten II	60.3	20.1	6055±46	6911	HG	
Varvarovka 15	48.8	36.7	4990±60	5745	F	TRUE
Vasil'evskij Kordon 5	53.0	40.4	6570±160	7458	un	TRUE
Vasil'evskij Kordon 7	53.0	40.4	5930±80	6767	un	

Site Name	Latitude	Longitude	DateBP (uncal) ± SD	Average date cal BP (INTCAL09)	Economy	Retained?
Veksa 3	59.3	40.2	6950±150	7803	HG	TRUE
Vela Spila VI	43.0	16.7	7300±120	8126	F	TRUE
Veluska Tumba	41.0	21.8	6912±64	7755	F	
Vepsänkangas	65.0	26.2	6170±90	7053	HG	TRUE
Veshchevo-1	60.9	29.5	5770±130	6583	HG	
Via Rivoluzione d'ottobre	44.7	10.6	6050±110	6922	F	
Viinikkala 2	60.3	24.9	5865±55	6682	HG	
Vilaggio A, Scaramella	41.5	15.7	7000±100	7830	F	
Villa	57.7	27.1	3570±240	3902	un	
Villa Communale	41.5	15.5	6850±130	7715	F	
Villaggio Rossi (Marcianese)	42.2	14.4	6590±130	7477	F	TRUE
Vinca	44.8	20.6	6190±60	7088	F	
Vinogradny Sad	47.8	31.2	4630±150	5307	un	
Vis 2	62.8	52.7	5370±90	6149	HG	TRUE
Vojmezhnoe 1	56.9	36.7	6550±100	7450	un	
Voronovitsy	48.4	26.5	6180±60	7079	F	
Voronovka II	47.4	31.0	5080±60	5816	un	
Vozhmarikha 26	62.1	35.2	6370±140	7274	HG	
Vrsnik-Tarinci	41.8	22.2	6892±62	7731	F	
Vulkaneshty II	45.7	28.4	5810±150	6633	un	TRUE
Wadi el Akhdar	23.2	26.0	9080±50	10245	HG	TRUE
Wadi Shaw 83/108	20.4	27.3	8470±50	9484	HG	TRUE
Wang	48.5	11.9	6181±60	7081	F	
Waremme-Longchamps	50.7	5.2	6295±69	7212	F	
Wegierce XII	52.8	18.2	5860±100	6677	F	
Weier	47.8	8.7	4846±65	5573	F	
Westeregeln	52.0	11.4	6104±67	6986	F	
Whitwell Long Cairn	53.3	-1.2	5209±48	5983	F	
Willerby Wold	54.2	-0.4	4930±106	5689	F	
Winden am See	48.0	16.8	5880±71	6696	F	
Windmill Hill	50.9	-1.9	4770±71	5488	F	
Winnall Down, Site R17	51.1	-1.3	4748±65	5468	F	
Wolla Bank	53.3	0.3	4865±65	5601	ME	

Site Name	Latitude	Longitude	DateBP (uncal) ± SD	Average date cal BP (INTCAL09)	Economy	Retained?
Wozna Wies I	53.8	22.8	5900±100	6732	HG	
Xianrendong Cave	28.7	117.2	17460±210	20815	HG	TRUE
Xinglongwa	42.4	120.8	7470±115	8273	F	TRUE
Yagoua, Cameroon	10.3	15.2	4010±110	4509	un	TRUE
Yanik Tepe	37.9	45.9	7035±69	7859	F	TRUE
Yankito	45.3	147.9	6980±50	7816	HG	TRUE
Yasinovatka	48.2	35.3	6357±40	7297	ME	
Yazykovo I	57.3	33.4	6950±70	7790	HG	TRUE
Ylikiiminki 46	60.0	26.2	6064±34	6919	HG	
Yuchanyan	25.5	111.5	14835±60	18132	HG	TRUE
Yumizh I	62.2	44.4	4320±40	4898	HG	TRUE
Yurtobor 3	57.2	67.0	9025±70	10152	HG	
Zadubravlje–Duzine	45.2	18.2	7610±140	8434	F	TRUE
Zage	49.9	35.8	7147±91	7971	un	TRUE
Zalany	50.6	30.9	5881±100	6710	F	
Zalavár	46.7	17.2	6180±100	7070	F	TRUE
Zales’ye I	57.0	33.3	6530±50	7443	un	
Zamost’e 2	56.7	38.1	7200±90	8037	HG	
Zan’kovtsi	48.8	38.5	7540±65	8336	ME	TRUE
Zapsė 5	54.2	23.4	4860±260	5579	ME	
Zarech'ye	49.4	24.1	5670±50	6453	un	TRUE
Zariza	49.2	42.5	4430±60	5069	un	TRUE
Zatsen'ye	54.2	27.5	5625±40	6397	un	
Zedmar A	54.7	22.0	5440±90	6211	HG	
Žemajtiške 3	55.3	26.1	5730±35	6529	HG	TRUE
Zengpiyan	28.3	110.3	10980±180	12888	HG	TRUE
Zhabki III	50.4	33.1	6870±100	7721	HG	
Zhalainuoer	49.4	117.6	7070±200	7917	HG	TRUE
Ziegelei Apfelthaler, Pulkau	48.7	15.9	6215±100	7107	F	
Zolotets IV	62.8	36.5	5160±150	5930	HG	TRUE
Zopy	49.3	17.6	6430±100	7344	F	TRUE
Zuojiashan	43.8	125.3	6755±115	7626	ME	TRUE

Site Name	Latitude	Longitude	DateBP (uncal) ± SD	Average date cal BP (INTCAL09)	Economy	Retained?
Zurich	47.4	8.6	5145±70	5883	F	
Zurich-Bauschanze	47.4	8.5	5320±60	6098	F	
Zvejnieki	56.3	25.1	6005±75	6854	HG	TRUE
Zwenkau-Harth	51.2	12.4	6001±43	6842	F	